Transient Electron Donor Concentration Experiments for the Determination of Dehalogenation Rate and Kinetic Parameter Shifts in an Anaerobic Microbial Culture

by
Jennifer K. Green

A PROJECT

submitted to

Oregon State University

University Honors College

in partial fulfillment of
the requirements for the
degree of

Honors Baccalaureate of Science in Environmental Engineering
(Honors Scholar)

Presented May 10, 2016
Commencement June 2016

AN ABSTRACT OF THE THESIS OF

Jennifer K. Green for the degree of Honors Baccalaureate of Science in Environmental Engineering presented on May 10, 2016. Title: Transient Electron Donor Concentration Experiments for the Determination of Dehalogenation Rate and Kinetic Parameter Shifts in an Anaerobic Microbial Culture.

Abstract approved:

_____

Lewis Semprini

Trichloroethene (TCE) is a common groundwater contaminant. Bioremediation, or the enhancement of natural microbial processes for the transformation of toxic compounds in soil and groundwater, is an effective solution to this widespread problem. The organisms that transform TCE in the subsurface are sensitive to environmental conditions, especially to the presence of an electron donor, which is required in the form of hydrogen (H_2) for the microbial processes to occur. This study explored the effects of electron donor concentration on TCE transformation rates of the anaerobic bacteria, *Dehalococcoides mccartyi*. Degradation rates of TCE and its transformation products were monitored for nine months following an increase in electron donor concentration within reactors maintaining mixed cultures of *D. mccartyi* at Oregon State University. Kinetic parameters representative of microbial transformation abilities were also monitored to develop conclusions regarding the community dynamics within the reactors.

Key Words: Trichloroethene, bioremediation, *Dehalococcoides*, electron donor

Corresponding e-mail address: jenniferkgreen17@gmail.com

Transient Electron Donor Concentration Experiments for the Determination of Dehalogenation Rate and Kinetic Parameter Shifts in an Anaerobic Microbial Culture

by
Jennifer K. Green

A PROJECT

submitted to

Oregon State University

University Honors College

in partial fulfillment of
the requirements for the
degree of

Honors Baccalaureate of Science in Environmental Engineering
(Honors Scholar)

Presented May 10, 2016
Commencement June 2016

Honors Baccalaureate of Science in Environmental Engineering project of Jennifer Green presented on May 10, 2016.

APPROVED:

Lewis Semprini, Mentor, representing Chemical, Biological, and Environmental Engineering

---

Mohammad Azizian, Committee Member, representing Chemical, Biological, and Environmental Engineering

---

Tyler Radniecki, Committee Member, representing Chemical, Biological, and Environmental Engineering

---

Toni Doolen, Dean, University Honors College

I understand that my project will become part of the permanent collection of Oregon State University, University Honors College. My signature below authorizes release of my project to any reader upon request.

Jennifer K. Green, Author

ACKNOWELDGEMENTS

I would first and foremost like to thank Dr. Lewis Semprini for being my research, academic, and thesis mentor for the past three years. It was an honor working for someone who cares equally about the research and the people doing it; I never went a summer in the lab without being treated to lunch, friendly conversation, and helpful advice. His constant words of encouragement and wisdom has armed me with a confidence in my own abilities, whether they be academic or otherwise, and I feel prepared to handle any challenges the future may hold. I hope the respect and gratitude I have for him and this experience is reflected in the work I present in this thesis.

I would like to thank Dr. Mohammad Azizian for being a member of my thesis committee and for being patient with me as I was learning to prepare experiments, work equipment, and analyze results. Without his diligence, talent, and kindness, absolutely nothing would get done in the lab. His efforts are appreciated more than he knows, and it has been a pleasure working with him. I would also like to thank Dr. Tyler Radniecki for being a member of my thesis committee and for providing me with valuable advice in and out of the classroom. From professional and graduate school advice to lectures on statistical data analysis, his efforts were greatly appreciated.

I would like to thank Stephanie Rich for the continuous support. She went above and beyond the call of duty as a mentor, colleague, and friend. Whether it was checking experiments, editing thesis and personal statement drafts, giving me advice on my future, or bringing me ice cream when I had the flu, she was always there to lend a helping hand. I am so grateful for the years of laughter, friendship, pizza, and acting ridiculous in public.

I would like to thank Kevin McKeage for teaching me so many valuable skills in the lab and always offering me advice and supplies. He made the often slow-paced and repetitive environment so much more bearable for everyone with his jokes and dancing, and it was deeply appreciated. I would also like to thank Kyle Vickstrom for being a great colleague as well as an all-around nice person. I wish him the best of luck with the rest of his graduate work, and may the force be with him.

Thank you, of course, to my family for the encouragement over the years. A special thank you to my mom for the unwavering emotional (and financial) support. She is an unstoppable force, bound and determined to provide for those around her. I promise to return the favor someday.

Finally, this research would not have been possible without funding. I was selected to be a first- and second-year intern for the Johnson Undergraduate Internship Program through the School of Chemical, Biological, and Environmental Engineering at Oregon State University. Pete and Rosalie Johnson generously donate their time and money to provide students with hands-on engineering research experience during the summer to improve all areas of their educational and professional careers. It is appreciated more than they know. I was also a registered contributor to the National Science Foundation MCB Grant No. 1330832 and was grateful for the opportunity to play a part in helping the grant and Foundation achieve their goals.

TABLE OF CONTENTS

LIST OF TABLES

LIST OF FIGURES

BACKGROUND

In the United States, chlorinated solvents have been widely used for dry cleaning and metal degreasing since the early 1900s. Trichloroethene (TCE), one of the best and most versatile of these solvents, became prevalent in the 1940s as a result of its ability to vapor degrease metal. In the 1960s however, environmental and health impacts associated with these compounds were made public, including the status of TCE as a possible human carcinogen. This sparked emission regulations in the 1970s and various classifications in the 1980s. The improper storage and disposal of chlorinated solvents lead to a widespread contamination issue, and various methods were developed for treatment (*1*). Unfortunately, these compounds are resilient and continue to persist in the environment today—nearly half a century after their introduction. As of 2011, TCE was also elevated in status to a known carcinogen, regardless of route, further articulating the need for its complete and safe remediation from a human health standpoint (*2*). Current remediation methods include *ex situ* pump-and-treat, flushing, air injection, *in situ* thermal and chemical technologies, and biodegradation (*1*). Biodegradation of chlorinated solvents is the focus of this study with an emphasis on degradation rate analysis.

Bioremediation

Biodegradation, more commonly referred to as bioremediation, is "the chemical breakdown of contaminant compounds by organisms, often microorganisms, and their associated metabolic processes" (*3*). The bioremediation of chlorinated solvents is a promising solution to an extremely widespread problem, utilizing naturally-occurring or artificially-enhanced processes to transform these dangerous compounds into less harmful or non-toxic products (*3*).

Traditional clean-up methods are less successful than bioremediation due to the chemical and physical properties of chlorinated solvents. TCE, a chlorinated aliphatic hydrocarbon (CAH), is liquid at room temperature and denser than water. CAHs sink deep into the subsurface forming dense nonaqueous phase liquids (DNAPLs) as they travel from a point source, through the saturated (vadose) zone, and into the groundwater within an aquifer.

Downward and horizontal movement of water through the subsurface saturated with a DNAPL dissolves the chlorinated solvents and forms a contaminated plume (*1*). This process is represented in Figure 1.

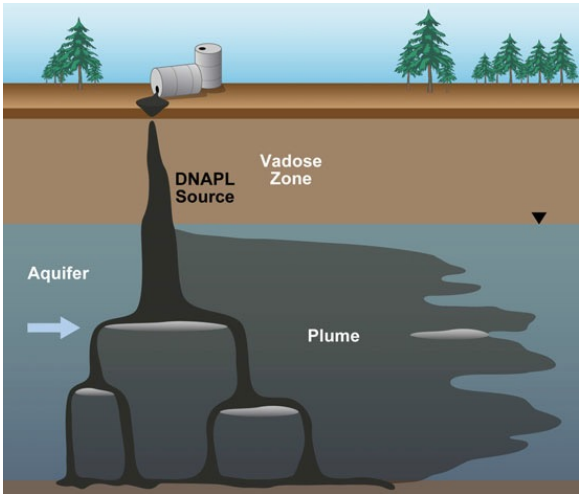

Figure 1. DNAPL from a point source can transverse the vadose zone and reach large sources of groundwater. Movement of water within the subsurface dissolves and transports the DNAPL, often to great distances from the point source (*1*).

The depths to which these compounds can reach are often anoxic and inhabitable to many organisms that rely on oxygen as their terminal electron acceptor, referred to as aerobic organisms. Anaerobic organisms utilize many compounds except oxygen as their terminal electron acceptor, including sulfate, carbon dioxide, nitrate, and iron. Some aerobic organisms have been shown to degrade CAHs in cometabolic processes where the organisms use a primary substrate for growth and energy while simultaneously transforming the chlorinated solvents (*4*).

However, slow and often incomplete dechlorination via cometabolism in the earliest investigations suggested that there were other processes at work—specifically the direct use of CAHs as primary substrates. In the beginning of the 1990s, anaerobic organisms were discovered that could grow using chlorinated ethenes as terminal electron acceptors in a respiratory process of reductive dehalogenation and showed faster rates of degradation compared to cometabolic processes (*3*). With the promise of faster remediation, ability to thrive in anoxic environments, and efficient utilization of CAHs as growth substrates, these

anaerobic organisms have become the subject of intensive research, including that which is presented in this study.

Reductive Dehalogenation

Reducing environments prefer a decrease in the oxidation state of the reactive chemical species within them and are generally void of oxygen. These environments exist on a relative scale in contrast with oxidative environments, ranging from most oxidizing to most reducing in order of energetically favored conditions. Anaerobic bacteria favor reductive processes shown in Figure 2 in preferential order from nitrate-reduction to methanogenesis. Reductive dehalogenation occurs at the strongly-reducing end of the scale (*3*). Finding organisms that favor these reductive processes is therefore critical to the effective implementation of any bioremediation effort to treat chlorinated solvents.

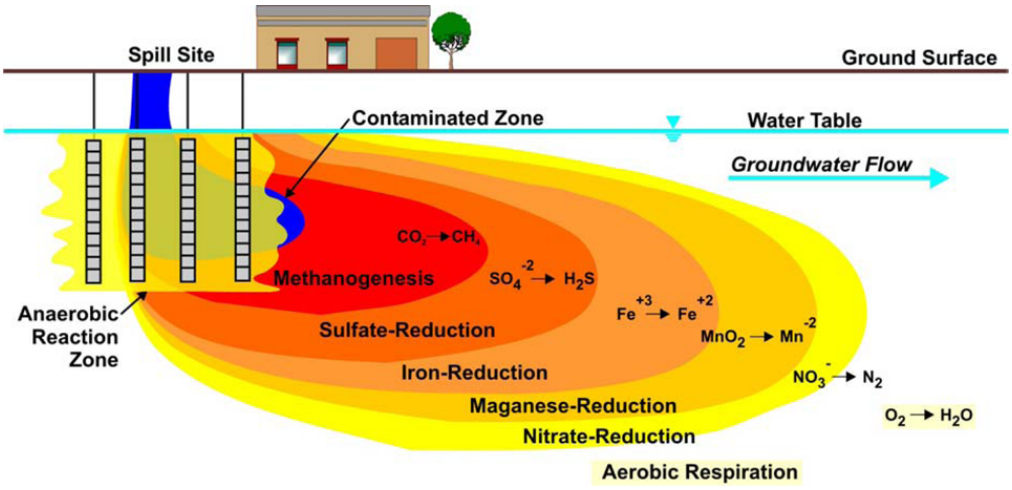

Figure 2. Reductive processes of anaerobic microorganisms in order of least energetically favorable (red) to most energetically favorable (yellow). Reductive dehalogenation is usually favored under methanogenesis (*5*).

Bacteria in a Mixed Culture

The bacteria species known as *Dehalococcoides mccartyi* favors the reductive dehalogenation process, using TCE as its primary substrate (electron acceptor) in a strictly anaerobic environment, making it an effective candidate for bioremediation and bioaugmentation (*6*). The basic reaction sequence by which TCE is converted to ethene (ETH) by *D. mccartyi* is presented in Figure 3.

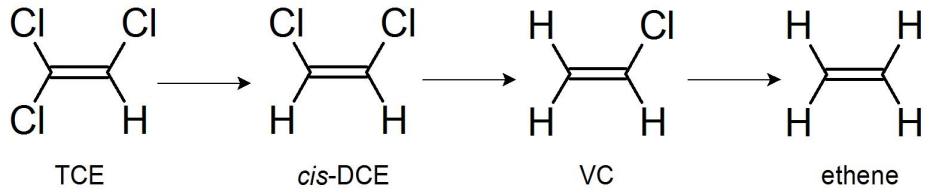

Figure 3. Reaction sequence for the conversion of TCE to ethene. *D. mccartyi* has the ability to completely transform TCE via reductive dehalogenation to produce *cis*-dichloroethene (*cis*-DCE), vinyl chloride (VC), and ethene, in this order.

The reaction sequence of TCE to ethene requires an electron donor in the form of hydrogen gas (H_2). Studies show that *D. mccartyi* cannot grow on its electron acceptor without H_2, present (*12*). The basic mechanism of each step from CAH to transformation product is presented in Figure 5.

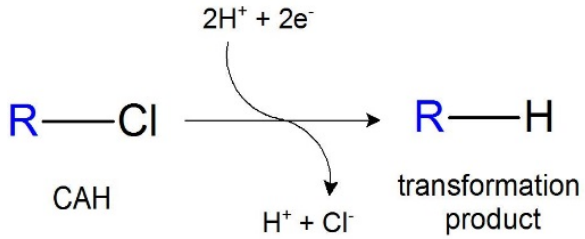

Figure 4. Chlorine is "replaced" with a hydride ion in each step of the reaction sequence of TCE to ethene. CAHs are sequentially transformed into less-chlorinated compounds using electrons supplied via H_2 gas.

Several proposed degradation pathways exist in an attempt to explain the process by which these organisms transform TCE predominantly via the *cis* isomer of dichloroethene (DCE), rather than via the *trans* isomer. Though a definitive conclusion regarding all reactions has yet to be reached, it is clear that the initial reaction step is catalyzed by cob(I)alamin in the reductive dehalogenase (*rdh*) genes present in *D. mccartyi* and similar microorganisms (*7*). Each *rdh* gene is responsible for a specific step in the transformation process: *rdh* gene *tceA* transforms TCE to VC while *vcrA* transforms VC to ethene (*6*).

In this study, *D. mccartyi* was cultured at Oregon State University in continuously-stirred tank reactors (CSTRs), referred to here as chemostats. Bacteria were maintained in mixed culture within the chemostats due to extensive studies showing *D. mccaryi* to be capable of faster dehalogenation rates and better growth when grown in mixed communities rather

than in isolation (*8*). Other community members potentially supply important growth factors and nutrients and, in return, *D. mccartyi* promotes fermentation reactions that produce H_2 and reduces toxicity by transforming TCE and other solvents (*8*). Three different mixed cultures of *D. mccartyi* and related organisms were grown in both two-liter (2L) and five-liter (5L) reactors for a total of six chemostats in operation. Substrate and electron donors could be varied between the two reactors for each culture to observe the dependence of degradation rate and inhibition on influent concentrations.

The Evanite mixed culture (EV) was obtained from a contaminated site near Oregon State University. The company formerly known as Evanite Fiber Corporation used a process involving large quantities of TCE to manufacture plastic battery separator material in Corvallis, OR. Improper disposal practices led to contamination in groundwater wells and nearby rivers. Pump and treat methods are currently employed in an attempt to contain the plume, but bioremediation has been introduced as a supplementary solution to the problem (*9*). The 2L reactor inoculated with EV culture taken from the banks of the nearby Willamette River (EV2L) was one focus of this project. The Victoria/Stanford mixed culture (VS) was originally sourced from the DuPont facility in Victoria, TX. Leachate from the industrial landfill on-site caused perchloroethene (PCE), TCE, *cis*-DCE, VC, and chloroethane contamination in the local aquifer (*10*). Studies using this culture were conducted at Stanford University to characterize the different bacterium species responsible for the conversion of PCE into ethene and to explore the factors that affect degradation rates (*11*). The 2L reactor inoculated with the VS culture grown at Stanford (VS2L) was another focus of this project.

Population data for these mixed cultures was generated by Dr. Alfred Spormann and his students at Stanford University. Polymerase chain reaction (PCR) methods were used to determine concentrations of *tceA*, *vcrA*, and *Dehalococcoides* spp. within each culture and provide insight into the relationship between gene expression and observed degradation capabilities (*12*). Recent data for EV2L, shown in Figure 5, indicated that the dominant *rdh* gene in the community was *tceA*, signifying a higher affinity for the dechlorination of TCE compared to the dechlorination of VC into ethene (*13*).

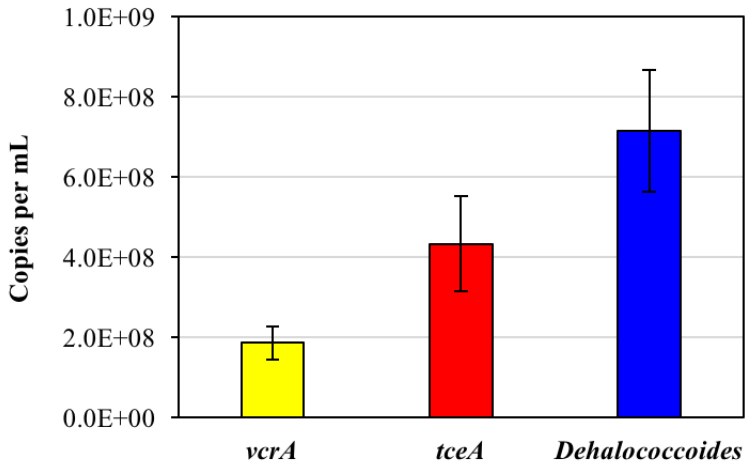

Figure 5. Results of 2013 qPCR analysis for EV2L culture. Enzyme concentrations indicated that the culture had a higher affinity for TCE transformation than VC transformation. VS2L was expected to exhibit similar population trends. Adapted from Spormann *et al.* (2014).

Two chemostats are still in operation for each mixed culture for variable growth condition experiments. The 5L chemostats have received excess electron donor via sodium formate (HCOONa) dehydrogenation or fermentation in solution to produce H_2, while 2L chemostats have received limited formate, causing performance and population dynamics of each culture to deviate for one another significantly (*15*). A summary of initial chemostat operating conditions is shown in Table 1. The 2L and 5L chemostats differ only in electron donor concentration; reactor volume is for identification purposes only.

Table 1. Summary of inoculum, electron donors, and electron acceptors for EV5L, EV2L, VS2L, and VS5L cultures. Adapted from Marshall *et al.* (2013).

		Electron Donor		**Electron Acceptor**	
Name	*Inoculum*	*Compound*	*Concentration*	*Compound*	*Concentration*
EV5L	Evanite	Formate	45 mM	TCE	10 mM
EV2L	EV5L	Formate	25 mM	TCE	10 mM
VS2L	Victoria/Stanford	Formate	25 mM	TCE	10 mM
VS5L	VS2L	Formate	45 mM	TCE	10 mM

The required H_2 concentration to completely transform 10 mM of TCE is 30 mM. It is 25.1 mM if TCE is assumed to be at the aqueous solubility limit of 1100 mg/L (*16*). See Appendix C for calculations. EV2L and VS2L are only slightly electron donor-limited from

a stoichiometric standpoint, but this is enough to cause a noticeable shift in reactor performance over time. In addition, homoacetogens and other co-culture organisms compete with *D. mccartyi* for H_2, further exacerbating restricted conditions (*17*).

Sodium formate is an indirect electron donor—it is converted to H_2 via microbial processes within the consortium. Studies suggest that fast-fermenting substrates like formate, or slow-fermenting substrates including propionate and butyrate, can all serve as indirect electron donors for the dehalorespiring species. The advantage of these soluble substrates over direct H_2 gas addition is that the *in situ* application is much simpler, and the distinct advantage of formate is that it self-neutralizes hydrochloric acid (HCl) produced from dechlorination reactions if the acetic acid production by co-culture organisms is kept at a minimum (*17*). Reactions involved in the use of formate as an electron donor in the dechlorination of TCE are summarized in Table 2. Formate is converted enzymatically to sodium bicarbonate and produces necessary H_2 for *D. mccartyi* to convert TCE to ethene. Sodium bicarbonate acts as a buffer to HCl produced in the dechlorination process (*18*).

Table 2. Summary of reactions involved in the use of sodium formate as the electron donor in TCE dechlorination processes. Adapted from Aulenta *et al.* (2006).

Formate dehydrogenation	$3HCOONa + 3H_2O \rightarrow 3NaHCO_3 + 3H_2$
Reductive dechlorination of TCE	$HC_2Cl_3 + 3H_2 \rightarrow C_2H_4 + 3HCl$
Acid neutralization	$3NaHCO_3 + 3HCl \rightarrow 3NaCl + 3CO_2 + 3H_2O$
Net reaction	$HC_2Cl_3 + 3HCOONa \rightarrow C_2H_4 + 3NaCl + 3CO_2$

Microbial Kinetics

Developed in 1949, Monod growth kinetics describe the exponential growth phase of microorganisms using an empirical mathematical model. The Monod equation, shown in Equation 1, relates the specific growth rate (μ) to the substrate concentration available (S). The maximum specific growth rate (μ_m) is the absolute maximum rate capable of the organism and is independent of the substrate concentration. The half-saturation constant, (K_S) is the concentration at which μ is exactly one-half μ_m (*19*).

$$\mu = \frac{\mu_m S}{K_S + S} \tag{1}$$

Some organisms experience substrate inhibition, where certain types or concentrations of substrate slow the growth rate of the organism by reducing the ability of enzymes to catalyze certain reactions. One type of inhibition is Haldane inhibition, which is incorporated into the Monod equation in Equation 2. The inhibition constant (K_I) is the concentration at which the substrate inhibits enzyme functions. A high K_I indicates a less inhibitive substrate (*20*).

$$\mu = \frac{\mu_m S}{K_S + S + \frac{S^2}{K_I}} \tag{2}$$

The rate of substrate utilization can be related to Monod growth kinetics using substrate material balances around the reactor of interest. The substrate mass balance for a batch reactor is shown in Equation 3. The biomass concentration (X) is the amount of viable cells within the reactor. Yield (Y) is defined as the ratio of biomass generated to the mass of substrate utilized for growth (*19*).

$$\frac{dS}{dt} = -\frac{\mu X}{Y} = -\left(\frac{1}{Y}\right)\left(\frac{\mu_m S}{K_S + S + \frac{S^2}{K_I}}\right) X \tag{3}$$

The maximum specific growth rate can be related to the maximum specific utilization rate (k_m) using yield. Maximum utilization rate ($k_m X$) can be experimentally determined by measuring the change in substrate concentration over time rather than by characterizing the yield and growth rates of the organism. The basis of all theoretical models used in this study is presented in Equation 4, which incorporates the maximum specific substrate utilization rate-yield relationship into the substrate mass balance on a batch reactor.

$$\frac{dS}{dt} = -\frac{k_m X S}{K_S + S + \frac{S^2}{K_I}} \tag{4}$$

Developing comprehensive and accurate predictive models is important for the advancement of bioremediation technologies. Coupled with hydrogeological and chemical transport models, these kinetic models can more accurately predict how different remediation plans will operate in a given contaminated site. The most complex kinetic model for dechlorination considers competitive inhibition, which is similar to Haldane inhibition in mathematical form, but accounts for a different type of enzymatic process in which the presence of a parent compound prohibits the production of one or more transformation products (*21*). This will be discussed further in Methods and Materials.

Yu *et al*. performed a study to determine kinetic parameters for this competitive inhibition model for the EV culture using sequential CAH equilibrations in batch reactors. Stepwise increases in CAH concentration were introduced to the culture over a short time period, and the rates of parent compound disappearance and daughter product production were measured at each concentration. Reactors were purged with mixed gas following each rate experiment, and a higher concentration of CAH was introduced along with H_2 gas.

Daughter product production rates were used predominately in kinetic parameter determination due to better sensitivity in concentration measurements. Models were fit to production rates versus concentration data according to Michaelis-Menton kinetics using non-linear least squares fitting. Values for k_m and K_S were changed using the Solver Add-In (Frontline Systems Inc.) in Microsoft® Excel® (*22*). Values determined by Yu *et al.* (2005) that served as a starting point in similar modeling procedures presented in this study are presented in Table 3. Low K_S values for TCE and *cis*-DCE indicate the inhibition of VC to ethene transformation in the presence of these two compounds.

Table 3. Kinetic parameters (± standard deviation) for EV2L determined by Yu *et al.* (2005) using a "multiequilibration method" of introducing stepwise CAH concentration increases to batch reactors and modeling daughter product production rates.

Parameter \ Substrate, *z*	TCE	*cis*-DCE	VC
$K_{S,z}$ (μM)	1.8 ± 0.4	1.8 ± 0.3	62.6 ± 2.4
$k_{m,z}$ (μmol/mg of protein/day)	125 ± 14	13.8 ± 1.1	8.1 ± 0.9

PROJECT DESCRIPTION

This project investigated the overall effects of increasing electron donor concentration in an anaerobic culture previously maintained in an electron donor-limited environment. The concentration of sodium formate in the influent media feed solution to the EV2L and VS2L chemostats was increased from 25 mM to 45 mM, and transformation rates were monitored over the course of nine months. These experiments are henceforth referred to as 'transient electron donor concentration experiments.' The objectives of these experiments were to:

1) observe the effects of increased electron donor concentration on TCE, *cis*-DCE, and VC transformation capabilities of the EV2L and VS2L cultures, and
2) determine if shifts in kinetic parameters representative of the EV2L culture have occurred since they were last determined and values were published.

Objective 1 was satisfied by quantifying transformation rates over time using batch kinetic tests to mimic chemostat capabilities. Trends were identified and transformation rates at the conclusion of transient electron donor concentration experiments were compared to current transformation rates for the EV5L and VS5L cultures maintained under excess electron donor conditions. It was anticipated that an increase in formate concentration would cause an immediate and significant increase in transformation rates for *cis*-DCE and VC, and potentially TCE.

Objective 2 was satisfied by developing an iterative method to derive values for the kinetic parameter known as the half-saturation constant (K_S) by initiating theoretical modeling analyses with published values for EV2L. The ability of the theoretical model to fit experimental data was quantified and used to determine if the new method was successful at estimating shifts in kinetic parameters. Population data and statistical data analyses were implemented to determine if the conclusions posited were justified. It was suspected that kinetic parameters have shifted over time in response to a shift in microbial communities within the mixed culture and that the most recent published values for VC transformation are no longer representative of the EV2L culture.

MATERIALS AND METHODS

Methods for working successfully with anaerobic cultures have been improved and perfected over the course of many years. In the Environmental Engineering Bioremediation Lab at Oregon State University, culture transfer methods, sample preparation procedures, and safety protocols have been established to ensure anaerobic conditions during experiments and safe working conditions for researchers. All methods presented are the efforts of Dr. Mohammad Azizian, Dusty R. V. Berggren, and many others. Original procedures were modified to accommodate laboratory supply issues and reduce the possibility of oxygen contamination.

Anaerobic Chemostat Operation

Chemostats (CSTRs) are used to grow and maintain EV2L and VS2L. Each chemostat consists of a feed solution reactor, syringe pump, chemostat reactor, effluent collection reactor, and sample extraction utility, as depicted in Figure 6. The chemostat is a 2-liter borosilicate glass media bottle (VWR International, Radnor, PA) fit with a Corning® GL45 3-hole delivery cap (Corning Inc., Corning, NY) and several lines of PEEK tubing (IDEX Health and Sciences, Oak Harbor, WA) for reactor pressurization, feed solution flow, and effluent flow.

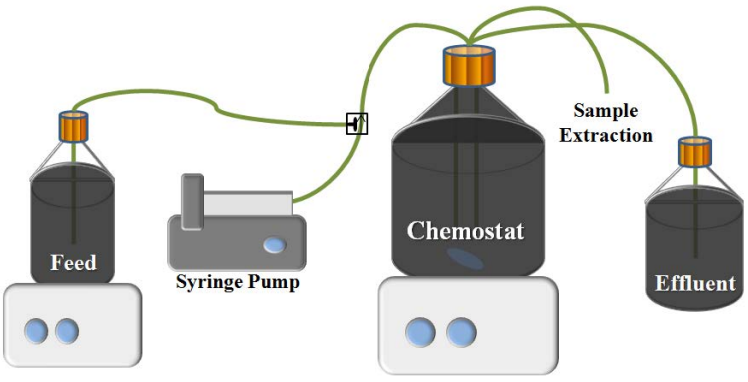

Figure 6. Basic chemostat configuration featuring chemostat reactor, sample extraction utility, feed and effluent reactors, and syringe pump. Feed and chemostat are mixed using stir plates (*21*).

Both cultures are fed anaerobic saturated TCE influent media—a solution of salts, minerals, sodium formate (H_2 source), sodium sulfide (O_2 buffer), and TCE at its aqueous

solubility limit (1100 mg/L). Resazurin, a redox-sensitive dye, is also added to indicate the presence of oxygen within the reactor and during culture transfers. Feed solution is contained in a 10-liter borosilicate glass media bottle (Corning Inc., Corning, NY) and used to refill a large glass gastight syringe on an Orion Sage® M361 syringe pump (Analytical Technology Inc., Collegeville, PA). Flow to chemostats is driven by the syringe pump set to maintain cell and hydraulic residence times of approximately 50 days (40 mL/day). Effluent is maintained anaerobically in a 2-liter borosilicate glass media bottle (VWR International, Radnor, PA) and is emptied periodically to ensure a constant flow rate through the chemostat. The sample extraction utility is a small length of PEEK tubing used to pressurize the chemostat with furnace-treated gas as described in a later section (see *Batch Kinetics Tests*). EV5L and VS5L chemostats are identical in operation, differing only in reactor size, composition of influent feed, and flow rate—a topic also addressed in a later section (see *Transient Electron Donor Concentration Experiments*). Procedures, protocols, and safety precautions taken with EV5L and VS5L are identical in all aspects to those described for EV2L and VS2L.

Batch Kinetic Tests

Batch kinetic tests were small-scale performance experiments to determine the maximum degradation rate capable of chemostat mixed cultures. These tests, run in triplicate, were prepared under strict anaerobic conditions to ensure reproducibility and longevity of transferred samples. Initial preparation began by placing three 125-mL clear borosilicate glass media bottles (Wheaton, Millville, NJ) and three phenolic screw caps with chlorobutyl rubber septa (Wheaton, Millville, NJ) into an anaerobic glovebox (90:10 N_2:H_2). Glass media bottles and caps with septa were autoclaved prior to use, and supplies were allowed to equilibrate within the glovebox for at least 24 hours. Caps were attached to all media bottles prior to removal from the glovebox to ensure an anaerobic environment.

Culture samples were transferred to glass media bottles using a positive pressure difference created between the desired chemostat and the anaerobic media bottle. Furnace-treated mixed gas (600 ºC, 75:25 N_2:CO_2) was fed to the desired chemostat, and PEEK tubing was attached to the glass media bottle using a sterile needle. PEEK tubing connections were

adjusted to direct flow, using the difference between the high pressure in the chemostat and atmospheric pressure in the media bottle to extract a sample. A 60-mL gas-tight syringe was also attached to the media bottle with a sterile needle to relieve pressure, catch hazardous compounds from the chemostat headspace, and ensure that the entire system remained anaerobic. A 50-mL culture sample was collected in each of the three glass media bottles. The 108-mL headspace of each sample was then purged of residual CAHs and ethene with the same furnace-treated mixed gas for approximately 15 minutes. Approximately 8 µmol of TCE and 100 µmol of H_2 (via sodium formate solution) was added to each media bottle immediately following the purging process.

Headspace concentrations of CAHs and ethene were monitored over time using an HP 6890 Series gas chromatograph (GC, Hewlett-Packard, Palo Alto, CA) fitted with a flame ionization detector (FID) utilizing helium as the carrier gas (15 mL/min) and a 30 m-0.53 mm GS-Q® column (Agilent Technologies, Santa Clara, CA). A Gastight model 1710 syringe (Hamilton Company, Reno, NV) was used to deliver 100-µL headspace samples to the FID. Batch reactors were incubated at 20 ºC and shaken on a shaker table at 200 RPM between headspace samples to ensure Henry's Law equilibrium was achieved. An example of experimental mass vs. time data is shown in Appendix D, Figure D1.

Transient Electron Donor Concentration Experiments

EV2L and VS2L were operated under limited electron donor conditions at 25 mM for several years to determine H_2 concentration effects on culture performance. Transformation rates were noticeably restricted and complete transformation of VC to ethene was never achieved in the chemostat; TCE was transformed to approximately 50% VC and 50% ethene. Transient electron donor experiments involved increasing the sodium formate concentration from 25 mM to 45 mM in both EV2L and VS2L chemostats and monitoring transformation rates over the course of several months using Batch Kinetic Test methods. CAH headspace concentration monitoring continued in order to observe improvements in VC conversion in the chemostat. Culture samples were also periodically taken for analysis by the team at Stanford to determine population shifts within EV2L and VS2L during experiments to corroborate observed rate trends.

Linear Rate Analysis

Linear rate analysis for batch experiments is based on the first principle of material balances. Mass accumulation is equivalent to the mass that enters, exits, is generated, and is consumed in a defined system. Kinetic tests were run under batch conditions, so mass did not enter, exit, or accumulate within the reactors. Mass consumption within the media bottle was equivalent to mass generation. Assuming no competitive inhibition of dehalogenation processes, material balances reduce to Equations 5, 6, and 7.

$$\text{TCE consumed} = \textit{cis}\text{-DCE, VC, and ethene produced} \quad (5)$$

$$\textit{cis}\text{-DCE consumed} = \text{VC and ethene produced} \quad (6)$$

$$\text{VC consumed} = \text{ethene produced} \quad (7)$$

This method of rate analysis utilizes these simple equations and linear regressions to determine the experimental transformation rate for each TCE, *cis*-DCE, and VC during batch kinetic tests based solely on mass data over time. The rate of degradation for each compound is equal to the rate of change, or linear regression slope, in the sum of the masses of all transformation products (as shown in Equations 5, 6, and 7). Rates are positive in this method of rate analysis because of the aforementioned mass balances and process of equating the mass of multiple compounds generated to the mass of one compound consumed. By convention, these degradation rates are also usually reported as positive values of mass of CAH transformed per unit volume and unit time.

For each data point, the mass of CAH is set equal to the sum of all transformation products at that point. The coefficient of determination (R^2) is calculated for each compound and non-linear points are deleted from the beginning and end of the data set until R^2 is greater than 0.98. A linear trend line is fit to the data and the slope is taken to be the maximum degradation rate in µmol/day. This rate is converted to units of µM/day for comparison purposes in later analyses. An example of this analysis applied to experimental data is shown in Figure 7.

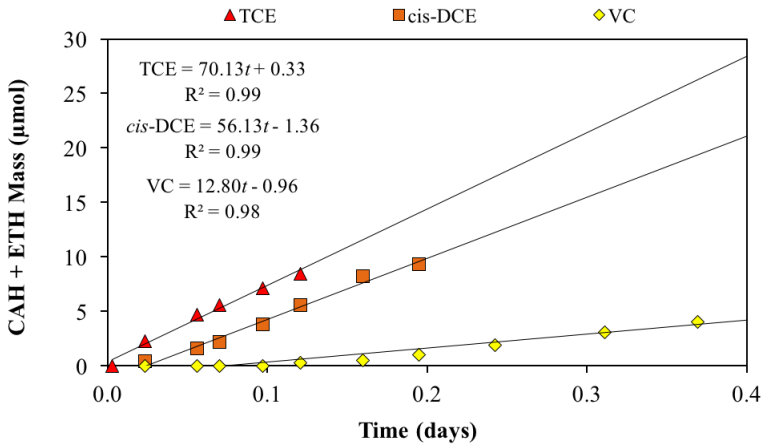

Figure 7. Example of linear rate analysis using experimental data. Linear trend lines are produced using built-in Excel® chart capability. Points at the beginning and end of data set were deleted as necessary to estimate the linear region of the experimental mass versus time data.

Multi-Fit Monod Model

Linear rate analysis assumes no competitive inhibition between substrate and transformation products, but there is qualitative and quantitative evidence that this is not the case with these cultures (*21, 22*). As a result, the simple material balances used to represent these processes do not account for inhibition and may underestimate the maximum transformation rates during batch kinetic tests. Linear rates are often lower than expected and can only be used as approximations.

A method of rate analysis was developed from the basic Monod equation to model the CAH transformation processes in anaerobic mixed cultures that includes inhibition (*21*). Numerical integration, statistical regression, and parameter fitting function simultaneously to predict CAH masses over time based on experimental data and determine the maximum specific utilization rate ($k_{m,z}$) and half-saturation constant ($K_{s,z}$) for any substrate z.

Developed by D. R. V. Berggren, the method known as the Multi-Fit Monod Model begins with an adapted form of the Monod kinetic equation, shown in Equation 8. The time rate of change of total reactor mass of substrate z (M_z) is dependent on the maximum specific utilization rate of z, the concentration of biomass in the batch kinetic test (X), the liquid concentrations of substrate z ($C_{L,z}$) and inhibitor y ($C_{L,y}$), the total liquid volume (V_L), the

half-saturation constant of z ($K_{S,z}$), and the inhibition constant of y ($K_{I,y}$). Inhibitors, y, are transformation products that delay or prevent the transformation of the parent compound. TCE, *cis*-DCE, and VC are all inhibitors during the transformation process (*21*).

$$\frac{dM_z}{dt} = \frac{k_{m,z} X C_{L,z} V_L}{K_{S,z}\left(1 + \frac{C_{L,y}}{K_{I,y}}\right) + C_{L,z}} \tag{8}$$

Berggren accounted for partitioning between liquid and gas phases within the system using Henry's Law and the unitless Henry's Law constant for substrate z ($H_{CC,z}$) to relate gas and liquid concentrations (C_L) (see Appendix B). The expression relating these concentrations, shown in Equation 9, was used to create a correction factor for simplification purposes. The correction factor ($K_{corrected,z}$ or $K_{cor,z}$) was used in the numerical integration process to reduce variables and is represented in Equation 10, where V_G is the total gas volume.

$$C_L = \frac{M_z}{V_L + V_G H_{CC,z}} \tag{9}$$

$$K_{cor,z} = K_{S,z}(V_L + V_G H_{CC,z}) \tag{10}$$

Berggren developed and simplified five equations using Euler's method for numerical integration that predict the mass of PCE and all transformation products for any time step (*21*). Because all batch kinetic tests in this study were conducted beginning with TCE, only equations for TCE and its daughter products are presented (Equations 11-14).

$$M_{TCE,t+\Delta t} = M_{TCE,t} - \frac{(k_{m,TCE} X) M_{TCE,t} V_L}{K_{cor,TCE} + M_{TCE}} \Delta t \tag{11}$$

$$M_{DCE,t+\Delta t} = M_{DCE,t} + (M_{TCE,t} - M_{TCE,t+\Delta t}) - \frac{(k_{m,DCE} X) M_{DCE,t} V_L}{K_{cor,DCE}\underbrace{\left(1 + \frac{M_{TCE,t}}{K_{cor,TCE}}\right)}_{\text{Inhibition term}} + M_{DCE}} \Delta t \tag{12}$$

$$M_{VC,t+\Delta t} = M_{VC,t} + \underbrace{\left(\frac{(k_{m,DCE}X)M_{DCE,t}V_L}{K_{cor,DCE}\left(1+\frac{M_{TCE,t}}{K_{cor,TCE}}\right)+M_{DCE}} \right)\Delta t}_{VC\ produced\ from\ cis-DCE\ transformation} - \underbrace{\left(\frac{(k_{m,VC}X)M_{DCE,t}V_L}{K_{cor,VC}\left(1+\frac{M_{TCE,t}}{K_{cor,TCE}}+\frac{M_{DCE,t}}{K_{cor,DCE}}\right)+M_{VC}} \right)\Delta t}_{TCE\ and\ cis-DCE\ inhibition\ of\ VC\ production} \quad (13)$$

$$M_{ETH,t+\Delta t} = M_{ETH,t} + \underbrace{\frac{(k_{m,VC}X)M_{VC,t}V_L}{K_{cor,VC}\left(1+\frac{M_{TCE,t}}{K_{cor,TCE}}+\frac{M_{DCE,t}}{K_{cor,DCE}}\right)+M_{VC}}\Delta t}_{TCE\ and\ cis-DCE\ inhibition\ of\ ETH\ production} \quad (14)$$

These equations were utilized in Microsoft® Excel® to compute, predict, and chart the results of the Multi-Fit Monod Model. Mass data over time was first added to the blank, pre-designed spreadsheet. The average system mass was calculated and used as the starting mass of TCE in the numerical integration (M_{TCE}). The prediction equations were already programmed into the spreadsheet and calculated masses for thousands of time steps immediately after an average mass was calculated for the system. VLOOKUP functions in Excel® matched the predicted data using numerical integration to experimental data based on time elapsed. The squared error between the experimental and predicted data was calculated and summed. Using the Solver Add-In (Frontline Systems Inc.), the sum of the squared errors (*SSE*) was minimized by changing k_mX, $K_{corrected}$ or both parameters simultaneously for each CAH (*21*). An example of this method of rate analysis applied to experimental mass vs. time data is shown in Appendix D, Figure D2.

SSE was minimized through a process of kinetic parameter optimization to ensure the theoretical model fit experimental data as accurately as possible. Optimization of these values was performed using an identical procedure each time to ensure consistency. First, the *SSE* was minimized by changing all k_mX values simultaneously without changing $K_{corrected}$ values. Next, the *SSE* was minimized by changing the k_mX and $K_{corrected}$ values for TCE simultaneously. The *SSE* was then minimized once more by changing all k_mX values simultaneously without changing $K_{corrected}$ values. This alternating process was repeated with *cis*-DCE and VC parameters. Starting values for k_mX and $K_{corrected}$ in Solver were always the final values from the previous test for that specific chemostat because of

limitations that exist in the software; Solver requires that the initial guess be fairly close to the actual value in order to successfully converge. Values for k_mX and $K_{corrected}$ were compared between triplicates for consistency. The exact process used to reach conclusions about kinetic parameter changes for the EV2L culture is explained in detail later (see *Kinetic Parameter Determination*).

This method of rate analysis operates on the basic assumption that there is constant biomass, which makes k_mX constant for each set of rate data. This assumption does not hold for longer, slower batch kinetic tests and the model often fails to fit experimental data. The tests performed in this study were relatively short in duration and were successfully fit with the Multi-Fit Monod Model to produce representative parameters for a specific culture at any given time. Values for k_mX in μM/day have been compared to converted linear rates to represent limitations and differences in rate analysis methods. This comparison also validates the converted rates from the linear rate analysis by showing their quantitative similarities and consistent trends.

RESULTS AND DISCUSSION

The objectives of this study were to 1) observe the effects of increased electron donor concentration on TCE, *cis*-DCE, and VC transformation rates in the EV2L and VS2L cultures, and 2) determine if shifts in kinetic parameters representative of the EV2L culture have occurred since they were last determined and values were published.

Chemostat Performance

CAH, ethene, acetate, and H_2 concentrations in reactors were measured regularly to monitor TCE to ethene conversion, which was not complete in the EV2L or VS2L reactors under limited electron donor conditions. Electron donor concentration in the influent saturated TCE media was increased from 25 mM to 45 mM at day 2684 of chemostat operation for EV2L and day 2378 for VS2L. Figure 8 shows the improved TCE to ethene conversion within the EV2L chemostat following the formate concentration increase (*23*). Steady state conditions were developed by day 2760, approximately. Figure 9 shows acetate and H_2 monitoring data for EV2L over the same time period (*23*). Increased acetate concentration indicates the stimulated growth of acetogens in the mixed culture as a result of increased H_2 concentrations. The presence of this co-culture organism can have an impact on electron donor availability to *D. mccartyi*.

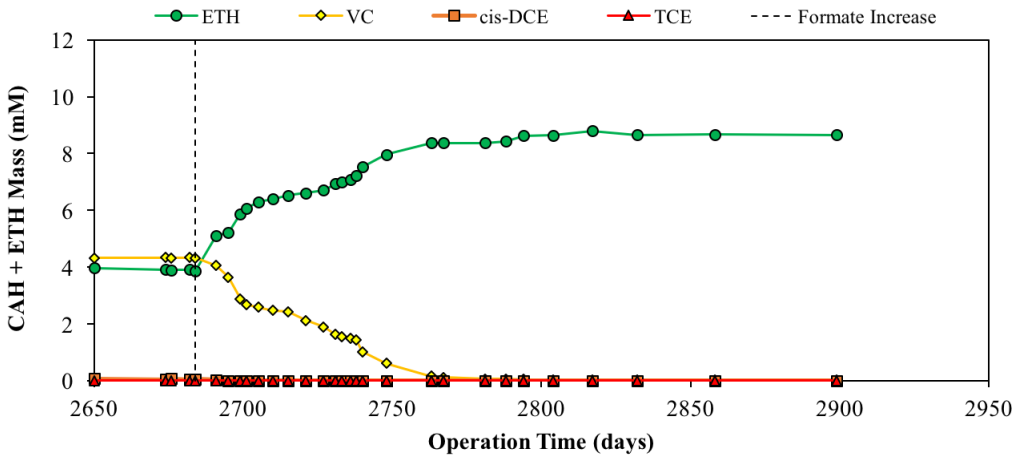

Figure 8. CAH and ethene concentration monitoring in EV2L during transient electron donor concentration experiments. More complete conversion of VC to ethene occurred immediately following the formate increase at 2684 days.

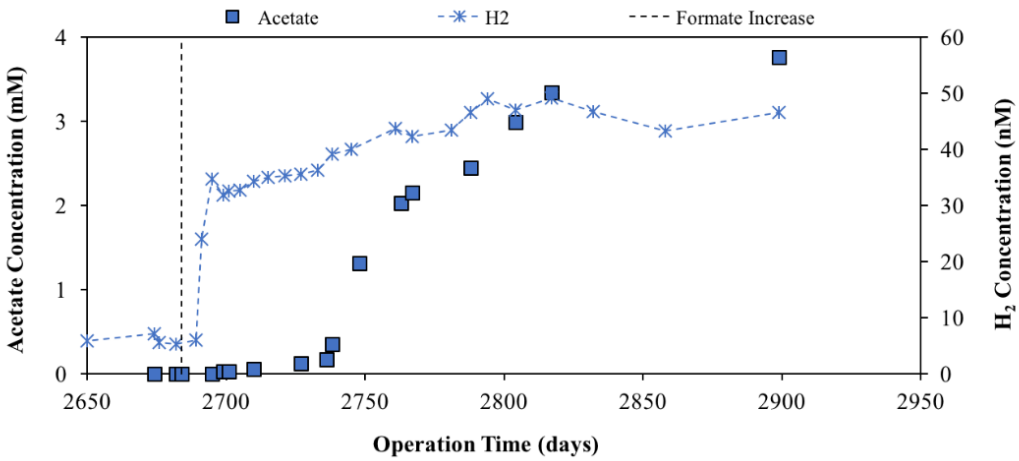

Figure 9. Acetate and H_2 concentration monitoring in EV2L during transient electron donor concentration experiments. Increased acetate production indicates stimulation of acetogen growth.

H_2 responds immediately to the increased formate concentration because it is present in the chemostat on a small scale (nM), however, acetate production is delayed. Concentrations begin to increase significantly after approximately 50 days, indicating that the delayed response is primarily due to CSTR kinetics. Chemostats maintain a 50 day hydraulic residence time. Both VS2L and EV2L responded similarly to the increase in formate concentration. Figure 10 shows the improved TCE to ethene conversion within the VS2L chemostat, where steady state conditions were developed by day 2460, approximately (*23*). Figure 11 shows acetate and H_2 monitoring data for VS2L over the same time period (*23*).

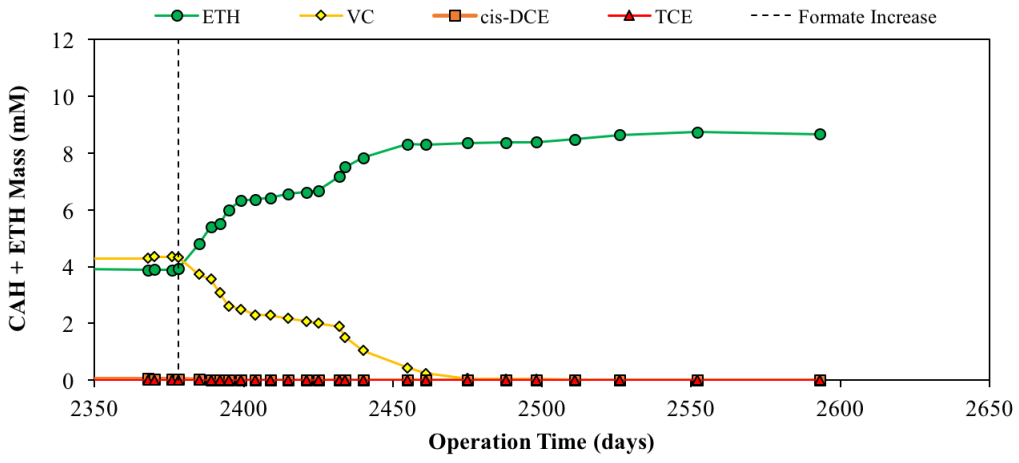

Figure 10. CAH and ethene concentration monitoring in VS2L during transient electron donor concentration experiments. More complete conversion of VC to ethene occurred immediately following the formate increase at 2378 days.

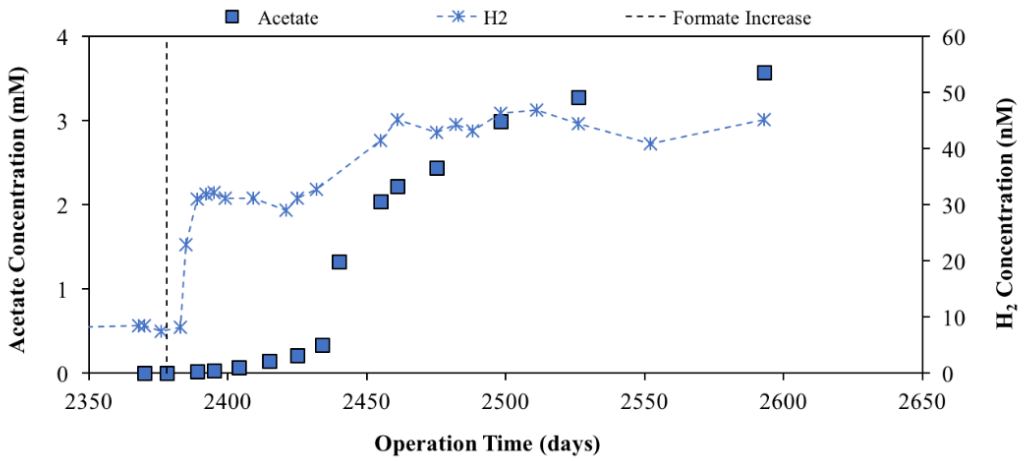

Figure 11. Acetate and H_2 concentration monitoring in VS2L during transient electron donor concentration experiments. Increased acetate and H_2 concentrations following the formate increase at 2378 days is the result of processes similar to those that occurred in the EV2L reactor.

Transient Electron Donor Concentration Experiments

An objective of this study was to investigate effects of electron donor concentration on transformation capabilities of EV2L and VS2L. CAH transformation rates during transient electron donor concentration experiments were determined using Batch Kinetic Test methods. Figure 12 shows average CAH k_mX values for EV2L during experiments. All k_mX values presented for both cultures were determined using the Multi-Fit Monod Model. A comparison of k_mX values with converted linear rates is shown in Appendix D, Figure D6.

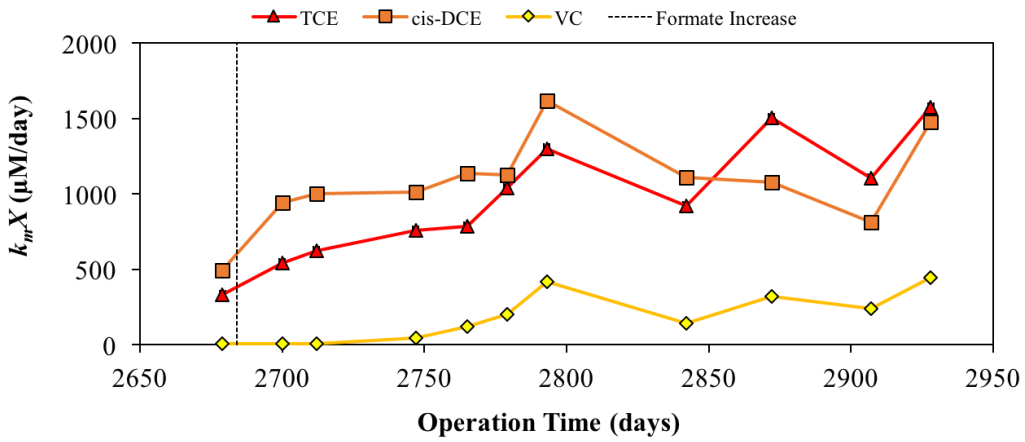

Figure 12. Average CAH k_mX values (µM/day) during transient electron donor experiments for EV2L. Compounds exhibit an initial increase in rates then stabilize at an approximate maximum. Figure D7 in Appendix D uses the theoretical model to visually show rates changing with time.

Figure D7 in Appendix D uses the theoretical model to visually show rates changing with time. All three compounds exhibited an increase in rate, then a stabilization at an approximate maximum. Table 4 summarizes initial CAH transformation rates for EV2L before the formate increase at day 2684 and the approximate maximum rates reached. TCE, *cis*-DCE, and VC rates increased by a factor of approximately 4, 2, and 80, respectively. The magnitude of increase in CAH rates and observed rate trends is interesting, especially in the case of TCE transformation. Prior to the formate increase at day 2684, TCE was completely transformed in EV2L. Complete transformation was still achieved during transient electron donor concentration experiments, but k_mX values increased, suggesting a shift in microbial population capable of more effective TCE transformation. This is supported by the observed exponential rate increase between days 2675 and 2800, which indicates the exponential growth of a strain of *D. mccartyi* within the mixed culture capable of more efficiently transforming VC to ethene, improving overall TCE transformation.

Table 4. Average CAH transformation rates for EV2L before formate increase and approximate maximum rates reached by the conclusion of experiments. Factors of increase and K_S values are approximate and take 95% confidence intervals for average k_mX values into consideration.

Parameter \ Substrate, *z*	TCE	*cis*-DCE	VC
k_mX before increase (μM/day)	333	493	5.0
Approx. Max k_mX (μM/day)	1500	1100	400
Factor of k_mX increase	4	2	80
Approx. K_S (μM)	2	0.9	6

Though not as pronounced, similar exponential growth can be observed in VS2L between days 2375 and 2475. This increase appears to occur more rapidly for VS2L, suggesting a more abundant initial population of efficient VC-reducing strains of *D. mccartyi* compared to EV2L. Similar rate increases and trends were also observed, as shown in Figure 13. 95% confidence intervals for average rates are not presented for simplicity, but support conclusions reached regarding rate changes. For rates determined between days 2450 and 2650, confidence intervals eliminate the large fluctuations observed, particularly for TCE and VC k_mX values at day 2580 and day 2575, respectively (see Appendix D, Figure D5).

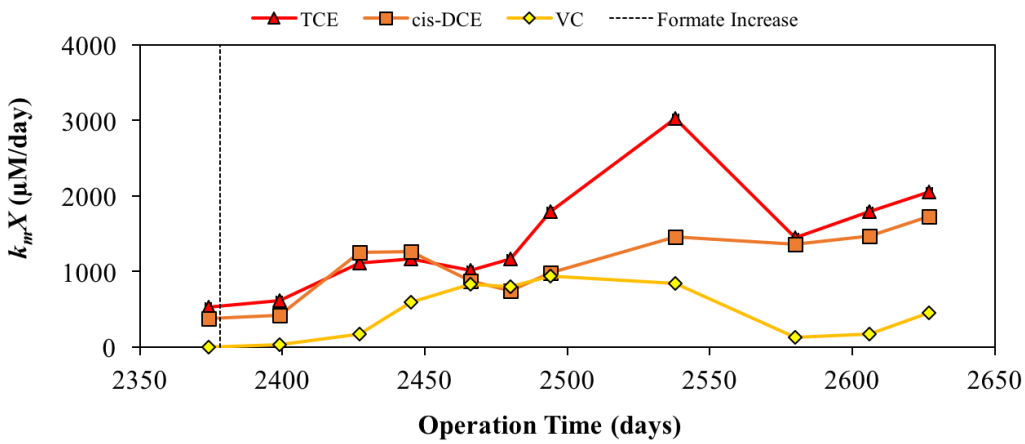

Figure 13. Average CAH k_mX values (µM/day) during transient electron donor experiments for VS2L. Rates fluctuated but generally increased with time, eventually reaching an apparent maximum. 95% confidence intervals (not shown) support this conclusion, especially for VC.

Table 5 summarizes initial CAH transformation rates for VS2L before the formate increase at day 2378 and the approximate maximum rates reached. TCE, *cis*-DCE, and VC rates increased by a factor of approximately 3, 4, and 400, respectively.

Table 5. Average CAH transformation rates for VS2L before formate increase and approximate maximum rates reached by the conclusion of experiments. Factors of increase and K_S values are approximate and take 95% confidence intervals for average k_mX values into consideration.

Parameter \ Substrate, *z*	TCE	*cis*-DCE	VC
k_mX before increase (µM/day)	527	376	1.6
Approx. Max k_mX (µM/day)	1700	1500	600
Factor of increase	3	4	400
Approx. K_S (µM)	10	3	30

Effects of formate increase on degradation rates were also analyzed by comparing 2L reactor rates before and after the formate increase to the most recent 5L reactor rates, as shown in Figures 14 and 15. Reactors of different volume were inoculated with the same culture, but maintained under different conditions (see Table 1 for complete details). Both reactors were continuously fed 10 mM TCE, but 5L reactors received 45 mM via feed solution, whereas 2L reactors originally received 25 mM.

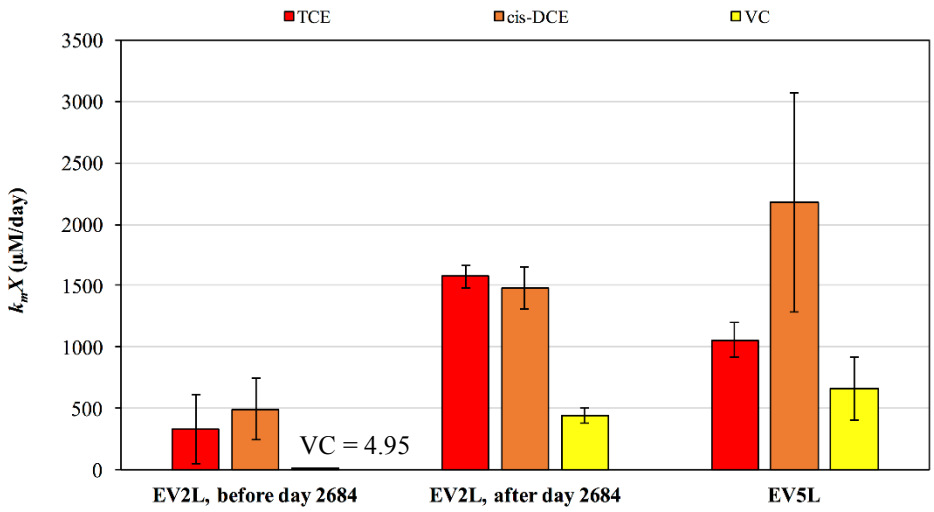

Figure 14. Comparison of k_mX values (µM/day) for EV2L before and after the formate increase at day 2684 with EV5L k_mX values. EV2L rates after the electron donor concentration increase were comparable to EV5L. Error bars represent 95% confidence interval.

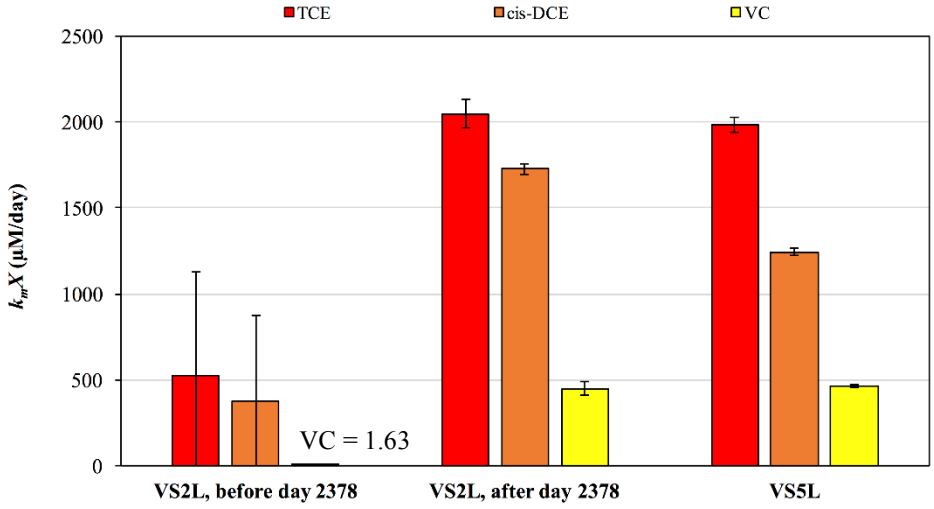

Figure 15. Comparison of k_mX values (µM/day) for VS2L before and after the formate increase at day 2378 with VS5L k_mX values. VS2L rates after the electron donor concentration increase were comparable to VS5L. Error bars represent 95% confidence interval.

2L reactor rates prior to the formate increase were substantially lower than 5L reactor rates, but following the increase, reactors were comparable. Acetate concentrations were also similar (see Appendix D, Figures D8 and D9). These results indicate that a shift in microbial population likely occurred, and a community was reestablished similar to that which exists in reactors maintained with excess electron donor. This is promising for field applications in the event of complications with electron donor substrate during treatment.

Kinetic Parameter Determination

The motivation behind kinetic parameter determination in this study was to explore an additional hypothesis fostered by the transient electron donor concentration experiments. It was suspected that a shift in the population of dehalogenating microorganisms has occurred in EV2L over recent years and that the half-saturation constant (K_S) has changed in response to this shift. The Multi-Fit Monod Model and published kinetic parameters served as the foundation for investigation.

Mathematical modeling and its results are theoretical. Validity relies on the logic and ethics of the method used to produce them. The use of Solver (Frontline Systems Inc.) in the Multi-Fit Monod Model introduces the possibility of unjustified attempts at finding parameters that make the model fit more accurately or produce desired results. A logical and systematic approach to determining these kinetic parameters was developed to ensure that the results of this modeling analysis truly indicate that a shift in K_S values has occurred.

Yu *et al.* developed a model using the Michaelis-Menton equation that incorporated the inhibition between CAHs within the anaerobic cultures (*22*). The EV culture was utilized in this study when it was grown in sequencing batch reactors on butanol, as compared to the current growth conditions within the two chemostats. The use of this culture in the development of the model simulation produced a set of kinetic parameters, including K_S, representative of the culture at that time. These published values, summarized in Table 6, served as the starting place for the investigation into whether there was a shift in the kinetic parameters for the EV2L culture.

Table 6. Direct K_S experiment results as determined by Yu *et al.* for the EV culture prior to chemostat inoculation (*22*). Values (± standard deviation) were determined for each individual substrate and used as initial values in Multi-Fit Model analysis on earliest experimental results.

Substrate, *z*	TCE	*cis*-DCE	VC
$\boldsymbol{K_{S,z}}$ **(µM)**	1.8 ± 0.4	1.8 ± 0.3	62.6 ± 2.4

The decision to use values published over a decade ago for a culture grown under completely different conditions was risky as they may no longer be entirely representative

of the current continuous cultures. However, kinetic parameters derived in the same study for Point Mugu (PM), a culture also grown and maintained in the laboratory at Oregon State University, were used by Berggren in 2011 for the development of the Multi-Fit Monod Model with much success (*21*). This suggests that the use of the published values with EV2L even after such a significant amount of time is justifiable for at least the beginning stages of the modeling process.

In general, the intention was to begin with early data sets, apply the values from Yu *et al.* to determine the kinetic parameters for that test, then utilize each new set of parameters in the modeling of subsequent batch kinetic tests. Consistency was valued above all else in this process to ensure that any observed trends could be presented with confidence. This new iterative approach to determining K_S began by using the published values in all parameter optimization analyses until Solver converged on a new solution, where both k_mX and K_S were allowed to vary together or separately. If Solver failed to converge on a solution, K_S values were held constant and only k_mX values were fit. If Solver converged on a solution and the sum of squared errors (*SSE*) in the Multi-Fit Monod Model was below a value of 5, the K_S values were averaged for the triplicates and used as the initial values in Solver for the subsequent test. Strict adherence to this procedure was followed and detailed notes were taken during analysis to ensure legitimacy and reliability.

Solver converged on a solution at the beginning of transient electron donor concentration experiments. New K_S values were only slightly different than published values, but new iterative methods were maintained, and K_S values for TCE, *cis*-DCE, and VC were monitored during transient experiments. TCE and *cis*-DCE K_S monitoring, shown in Figure 16, revealed slight fluctuations, but values did not deviate drastically from the published values. The same reductase enzyme is responsible for TCE and *cis*-DCE transformations, so similar trends in parameter shifts was expected. No extreme changes in K_S values suggests that the *tceA* reductase enzyme was not affected when EV2L was maintained under electron donor limited conditions. This is particularly interesting considering TCE and *cis*-DCE rates increased by factors of approximately 4 and 2, respectively.

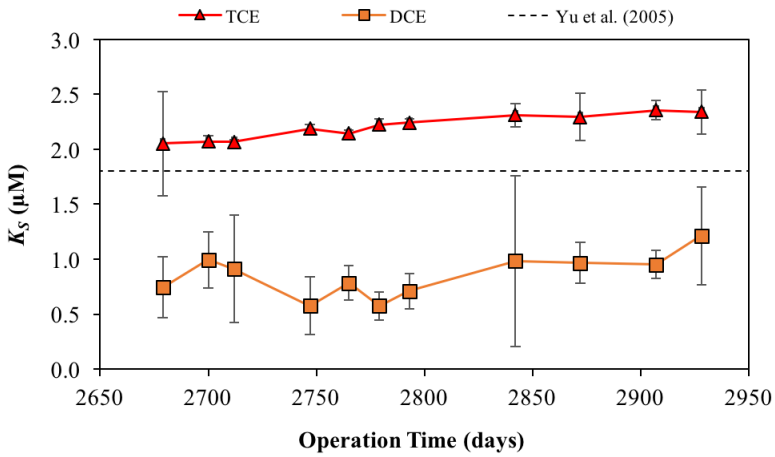

Figure 16. Average TCE and *cis*-DCE K_S values remained approximately constant over the course of transient electron donor concentration experiments and have not changed since they were measured by Yu *et al.* in 2005. Values were derived using the new iterative approach. Error bars represent 95% confidence interval.

VC K_S monitoring, shown in Figure 17, was more telling. The value determined before transient electron donor concentration experiments began was possibly high and approximately the value published by Yu *et al.* (2005). The K_S value may have decreased as experiments progressed. Overall trends indicate that the VC K_S value is lower now than when it was measured by Yu *et al.* (2005). Whether this value shifted as a result of the new environmental conditions cannot be determined.

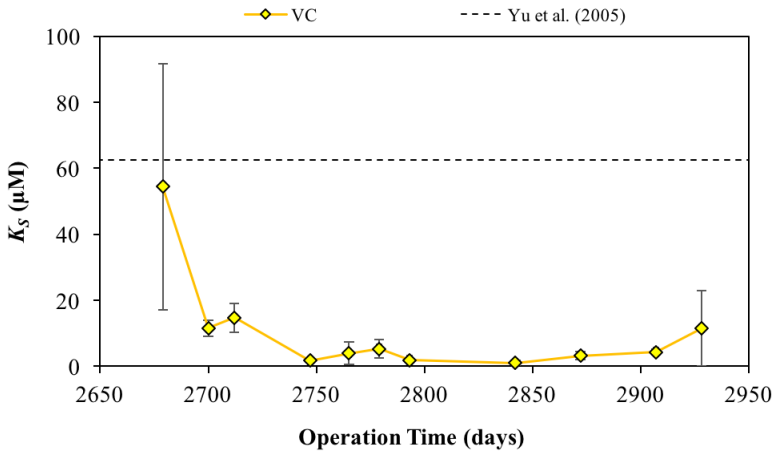

Figure 17. Average VC K_S values may have decreased during transient electron donor concentration experiments. Results suggest that K_S values have decreased since they were measured by Yu *et al.* in 2005. Values derived using new iterative approach. Error bars represent 95% confidence interval.

Table 7 compares values determined by Yu *et al.* with values determined using the new iterative approach based on results of the most recent batch kinetic tests. At the conclusion of the transient experiments, average TCE and *cis*-DCE K_S values fell within the error range for published values, suggesting no shifts since 2005 or over the course of the nine-month experiments. The average VC K_S value is approximately one-fifth of published values.

Table 7. Comparison of K_S values from Yu *et al.* (± standard deviation) with values determined using new iterative approach (± 95% confidence interval). Confidence interval for VC is large due to one measured value being much lower than the other two triplicates.

Source of $K_{S,z}$ \ Substrate, z	TCE	*cis*-DCE	VC
Yu *et al.* (2005)	1.8 ± 0.4 μM	1.8 ± 0.3 μM	62.2 ± 2.4 μM
Batch kinetic test, day 2928	2.3 ± 0.2 μM	1.2 ± 0.4 μM	11.4 ± 11.4 μM

The average VC K_S value for EV2L is comparable to published values for the VS culture (*24*). Haston and McCarty (1999) measured a VC K_S value (± 95% confidence interval) for the VS culture of 2.6 ± 1.9 μM. These values are even more dated than those measured for EV, but it is encouraging that a similar culture once exhibited K_S values within the 95% confidence interval predicted in this study.

Because the new iterative approach is an indirect method for determining K_S values, the actual quantities presented may not be as accurate as the direct measurements of Yu *et al.* (2005). Support for the suggested shift in VC K_S values comes from observation and characterization of model fitting. The Multi-Fit Monod Model relies on the statistical method of non-linear least squares fitting to determine kinetic parameters by minimizing the *SSE*. Comparing these values among models can suggest improved fitting. Observation of how well model-contrived data fits the entire data set as well as certain parts of the data set can corroborate conclusions reached from comparing *SSE* values.

To demonstrate the improved fitting using K_S values determined via the new iterative approach, data for the batch kinetic test on day 2928 was modeled with both sets of kinetic parameters given in Table 7. The Multi-Fit Monod Model was run with Yu *et al.* K_S values held constant, and again using the new iterative approach to initiate Solver using K_S values

from the previous batch kinetic test. Results were graphed simultaneously to determine key areas of deviation from experimental data. VC to ethene transformation proved to be most affected by the different K_S values. As suspected, the new K_S values provided a better fit than the values of Yu *et al.* (2005). Figure 18 shows the modeling method comparison for one triplicate of the batch kinetic test from day 2928, where the improved fit can be observed in the low VC masses at approximately 0.6 days.

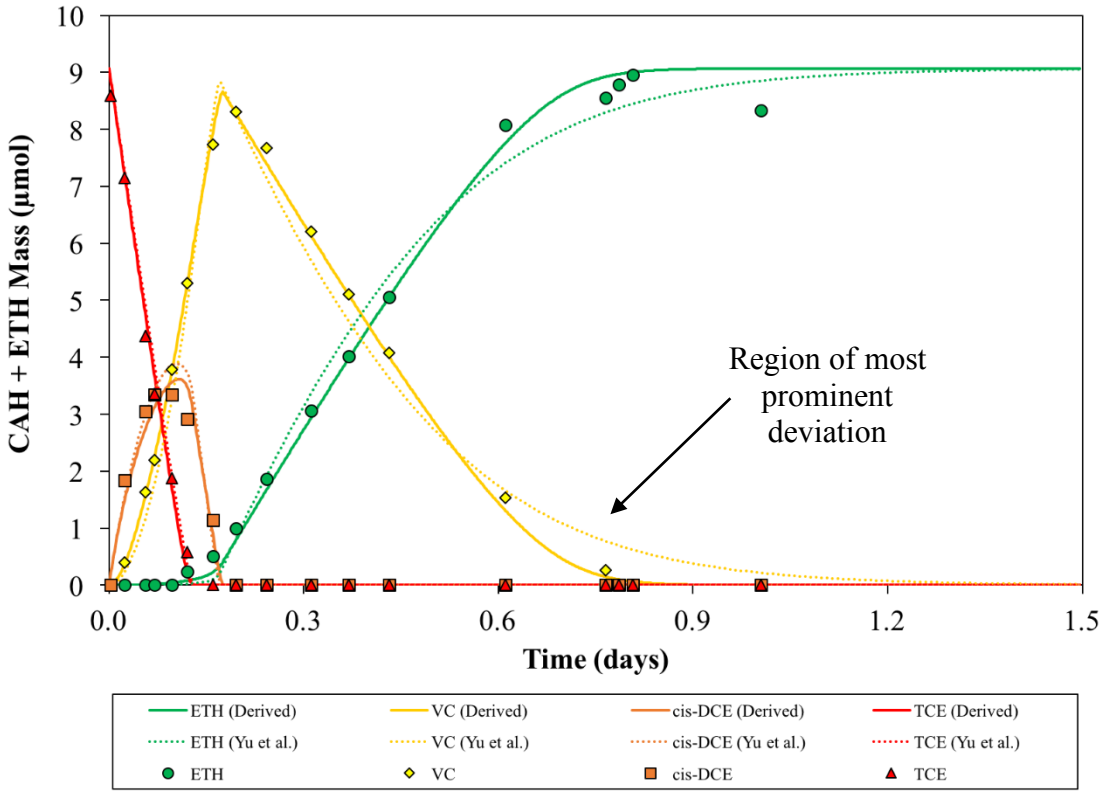

Figure 18. Model fitting comparison for one triplicate of batch kinetic test with EV2L. "Derived" designates fitting done using K_S values determined using new iterative approach. "Yu et al." designates fitting done using K_S values determined by Yu *et al.* (2005). Derived K_S values fit experimental data much more accurately, suggesting a shift in kinetic parameters for EV2L.

Newly-derived values clearly fit experimental data more accurately. Results indicate that the new iterative approach is an effective method for kinetic parameter determination. Results also indicate that VC K_S values have likely changed since 2005. Comparing *SSE* values for all three triplicates from the batch kinetic test on day 2928 supports the same conclusions. Table 8 compares the average *SSE* values between the two approaches.

Table 8. Comparison of average *SSE* values produced from modeling with derived K_S values and K_S values published by Yu *et al.* (2005). Values derived using the new iterative approach are much smaller, suggesting better fitting with this method.

Method	Yu *et al.*	Derived
Average model *SSE*	5.67	2.98
95% CI	± 3.01	± 1.06

Comparing k_mX values determined using the two different modeling approaches with converted linear rates also supports the legitimacy of the new iterative approach. Linear rates should always be lower than k_mX values determined using the Multi-Fit Monod Model because the linear method does not account for the location of the maximum rate or inhibition between substrates. Relative trends between CAHs should be consistent, however; if TCE rates are higher than *cis*-DCE rates using the linear rate analysis, TCE rates should be higher than *cis*-DCE rates using the Multi-Fit Monod Model.

Figure 19 shows the comparison of the average converted linear rate with the average k_mX determined using the Multi-Fit Monod Model with published K_S values held constant for the batch kinetic test on day 2928. TCE rates are comparable, but *cis*-DCE and VC rates are significantly higher using the model.

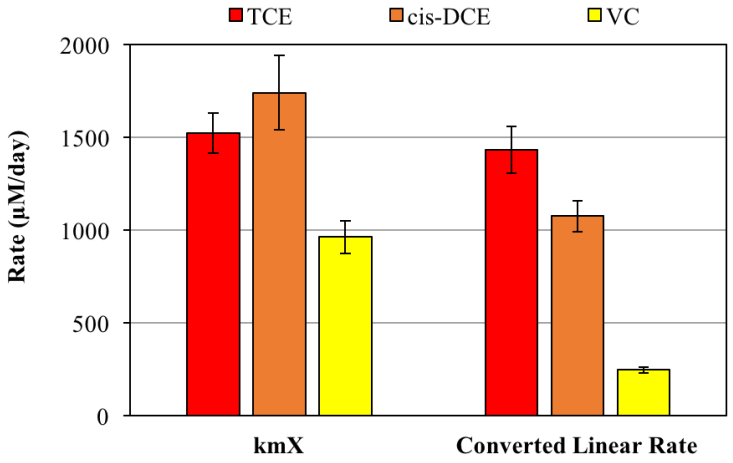

Figure 19. Average converted linear rates for batch kinetic test from day 2928 compared to average k_mX values determined by keeping K_S constant in model at values published by Yu *et al.* (2005). TCE rates are comparable but there is significant deviation between rate analyses for *cis*-DCE and VC rates. Error bars represent 95% confidence intervals.

Figure 20 shows the comparison of the average converted linear rate with the average k_mX determined using the new iterative approach in the Multi-Fit Monod Model. Rates for all CAHs are comparable between the two different rate analyses and trends between CAHs are preserved, further supporting the accuracy of the new iterative approach. TCE rates are greater than *cis*-DCE rates, and *cis*-DCE rates are higher than VC rates for both model and linear methods, but this was not true when the model was run with Yu *et al.* (2005) values.

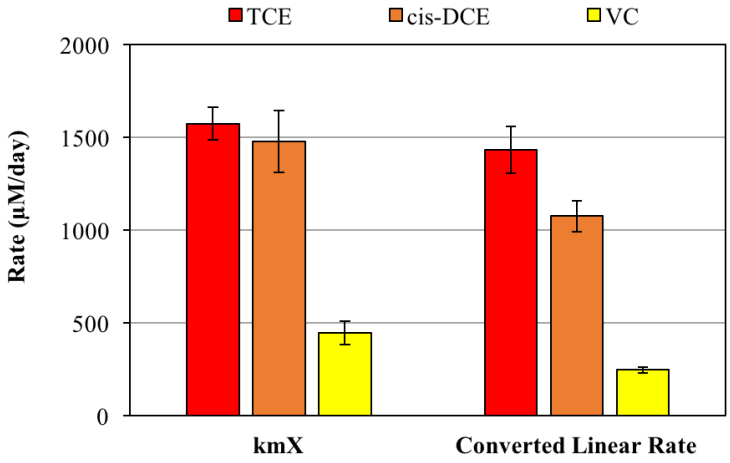

Figure 20. Average converted linear rates for batch kinetic test from day 2928 compared to average k_mX values derived using new iterative approach. Error bars represent 95% confidence intervals. Rates for all CAHs are comparable between different rate analyses and trends are preserved. TCE > *cis*-DCE > VC for both methods. Modeling with Yu *et al.* (2005) did not preserve this trend.

The legitimacy of the new iterative approach is supported equally by lower *SSE* values, better observed model fitting, and more accurate rate determination when compared with converted linear rates. The conclusion that the K_S value for VC has shifted since the parameter was last determined experimentally is supported with K_S monitoring over time using the new iterative approach. It can also be corroborated with recent results of molecular analyses by Koshlan Mayer-Blackwell, Ph.D. at Stanford University. The VC dechlorination is believed to be driven by the *vcrA* population, and there is data to support a K_S between 2.5 and 10 µM (*25*). Further statistical analyses will be performed to confirm the results of new modeling methods and solidify conclusions about these parameter shifts for a separate publication.

CONCLUSION

Trichloroethene (TCE) is a notoriously persistent contaminant in the subsurface. Many physical and chemical treatment technologies exist to remove TCE and related compounds from soil and groundwater, but biological treatment methods are an equally effective solution to an extremely widespread problem. Bioremediation is one biological treatment method, utilizing naturally-occurring or artificially-enhanced microbial processes to transform dangerous compounds into non-toxic end products.

Reductive dehalogenation is the transformation process by which TCE is reduced to ethene in the subsurface. In order for bioremediation to be effective, microorganisms should energetically favor this reductive dehalogenation process. One such organism is *Dehalococcoides mccartyi*—the only organism known to use TCE as its primary substrate and anaerobically transform it to *cis*-dichloroethene (*cis*-DCE), vinyl chloride (VC), and ethene. *D. mccartyi* is cultured in several mixed cultures within anaerobic chemostats at Oregon State University. Evanite (EV) and Victoria/Stanford (VS) cultures were the focus of this study, where each culture is still grown in both two-liter (EV2L, VS2L) and five-liter (EV5L, VS5L) reactors. Two-liter reactors have been maintained under limited electron donor conditions for nearly 8 years, and five-liter reactors have been maintained under excess electron donor conditions. A competitive inhibition model describe the growth and substrate utilization of these bacteria in mixed culture. Kinetic parameters of interest within this model include the maximum utilization rate (k_mX) and the half-saturation constant (K_S).

This project, as part of the National Science Foundation (NSF) Molecular and Cellular Biosciences (MCB) Grant No. 1330832, investigated the overall effects of increasing electron donor concentration in an anaerobic culture previously maintained in an electron donor-limited environment. The first objective of this project was to observe the effects of increased electron donor concentration on TCE, *cis*-DCE, and VC transformation capabilities of the EV2L and VS2L cultures. The second objective was to determine if shifts in the K_S value representative of EV2L culture substrate utilization have occurred since they were last measured by Yu *et al.* (2005).

Transient electron donor concentration experiments involved increasing the electron donor concentration in the feed solution for EV2L and VS2L reactors and monitoring transformation rates over time using batch kinetic tests. Gas chromatography determined the mass of TCE and its transformation products over time within small batch reactors containing culture from each chemostat, saturated TCE, and excess electron donor. Transformation rates were determined for each batch kinetic test using a linear rate method based on material balances and a numerical integration method based on a competitive inhibition Monod model.

Monitoring TCE and transformation product mass over time within each chemostat revealed a gradual improvement in TCE to ethene conversion from approximately 50% to 100%. Both EV2L and VS2L reached steady state in less 100 days after the increase in electron donor concentration. Monitoring transformation rates over the same time using batch kinetic test methods showed that TCE, *cis*-DCE, and VC rates increased by factors of 4, 2, and 80, respectively, in the EV2L culture and by factors of 3, 4, and 400, respectively, in the VS2L culture. All 2L reactor rates were comparable to 5L reactor rates determined during the same time period. Results indicate that a shift in the microbial population likely occurred, and a community was reestablished similar to that which exists in reactors maintained with excess electron donor. This is promising for field applications in the event of complications with the electron donor substrate during treatment.

Monitoring TCE and transformation product K_S values over time within each chemostat was done by applying the Multi-Fit Monod Model to batch kinetic test data and deriving new values based on the results of Yu *et al*. (2005). TCE and *cis*-DCE K_S values did not show significant deviation from values measured by Yu *et al.* (2005), which is interesting considering the increase in k_mX values observed for these compounds. However, VC K_S values are approximately five times lower than values measured by Yu *et al.* (2005), indicating a shift in the microbial population responsible for VC degradation and a higher affinity for culture growth at low VC concentrations. Shifts are also consistent with results of molecular analyses that also indicate an increase in populations containing *vcrA*—the enzyme responsible for VC transformation in *D. mccartyi*.

REFERENCES

(1) McCarty, P. L. Chapter 1 – Groundwater Contamination by Chlorinated Solvents: History, Remediation Technologies, and Strategies. In *In Situ Remediation of Chlorinated Solvent Plumes*; Stroo, H. F., Ward C. H., Eds.; Springer: New York, 2010; pp 1-28.

(2) *Toxicological Review of Trichloroethylene (CAS No. 79-01-6)*; EPA/635/R-09/011F; U. S. Environmental Protection Agency (EPA), Integrated Risk Information System (IRIS), U.S. government Printing Office: Washington, DC, 2011.

(3) Bradley, P. M.; Chapelle, F. H. Chapter 3 – Biodegradation of Chlorinated Ethenes. In *In Situ Remediation of Chlorinated Solvent Plumes*; Stroo, H. F., Ward C. H., Eds.; Springer: New York, 2010; pp 39-67.

(4) Semprini, L. Strategies for the aerobic co-metabolism of chlorinated solvents. *Curr. Opin. Bioctechnol.* **1997**, *8* (3), 296-308.

(5) Parsons Corporation. *Principles and Practices of Enhanced Anaerobic Bioremediation of Chlorinated Solvents*; 022/738863/28; Parsons Corporation: Los Angeles, CA, August 2004.

(6) Löffler, F. E.; et al. *Dehalococcoides mccartyi* gen. nov., sp. nov., obligately organohalide-respiring anaerobic bacteria relevant to halogen cycling and bioremediation, belong to a novel bacteria class, *Dehlococcoidia* classis nov., order *Dehalococcoides* ord. nov. and family *Dehalococcoidaceae* fam. nov., within the phylum *Chloroflexi*. *Int. J. Syst. Evol. Microbiol*. **2013**, *63* (2), 625-635.

(7) Cretnik, S.; Bernstein, A.; Shouakar-Stash, O.; Löffler, F.; Elsner, M. Chlorine Isotope Effects from Isotope Ratio Mass Spectrometry Suggest Intramolecular C-Cl Bond Competition in Trichloroethene (TCE) Reductive Dehalogenation. *Molecules*. **2014**, *19* (5), 6450-6473.

(8) Men, Y.; Seth, E. C.; Yi, S.; Allen, R. H.; Taga, M. E.; Alvarez-Cohen, L. Sustainable Growth of *Dehalococcoides mccartyi* 195 by Corrinoid Salvaging and Remodeling in Defined Lactate-Fermenting Consortia. *Appl. Environ. Microbiol.* **2014**, *80* (7), 2133-2141.

(9) Hall, B. Evanite cleanup entering new phase. *Corvallis Gazette-Times*, May 28, 2015.

(10) *EPA Environmental Engineering Sourcebook*; Boulding, J. R., Ed.; CRC Press: Boca Raton, 1996.

(11) Final Report: Mechanisms, Chemistry, and Kinetics of Anaerobic Degradation of cDCE and Vinyl Chloride. https://cfpub.epa.gov/ncer_abstracts/index.cfm/fuseaction/display.abstractDetail/abstract/2059/report/F (accessed April 13, 2016), online summary of project objectives and grant information.

(12) Mayer-Blackwell, K.; *et al.* A Nanoliter qPCR Platform for Highly Parallel, Quantitative Assessment of Reductive Dehalogenase Genes and Populations of Dehalogenating Microorganisms in Complex Environments. *Environ. Sci. Technol*. **2014**, *48* (16), 9659-9667.

(13) Spormann, A. M.; *et al.* Stanford University, Stanford, CA. Unpublished work, 2014.

(14) Maymó-Gatell, X.; Chien, Y.; Gossett, J. M.; Zinder, S. H. Isolation of a Bacterium That Reductively Dechlorinates Tetrachloroethene to Ethene. *Science*. **1997**, *276* (5318), 1568-1571.

(15) Marshall, I. P. G.; Azizian, M. F.; Semprini, L.; Spormann, A. M. Inferring community dynamics of organohalide-respiring bacteria in chemostats by covariance of *rdhA* gene abundance. *FEMS Microbiol. Ecol.* **2013**, *87* (2), 1-13.

(16) CLU-IN: Trichloroethylene (TCE) Chemistry and Behavior. https://clu-in.org/contaminantfocus/default.focus/sec/Trichloroethylene_(TCE)/cat/Chemistry_and_Behavior/ (accessed April 12, 2016), online summary of physical and chemical characteristics of TCE prepared by the EPA using peer-reviewed journals and books.

(17) Azizian, M. F.; Marshall, I. P. G.; Behrens, S.; Spormann, A. M.; Semprini, L. Comparison of lactate, formate, and propionate as hydrogen donors for the reductive dehalogenation of trichloroethene in a continuous-flow column. *J. Contam. Hydrol.* **2010**, *113*, 77-92.

(18) Aulenta, F.; Majone, M.; Tandoi, V. Enhanced anaerobic bioremediation of chlorinated solvents: environmental factors influencing microbial activity and their relevance under field conditions. *J. Chem. Technol. Biotechnol.* **2006**, *81*, 1463-1474.

(19) Shuler, M. L.; Kargi, F. *Bioprocess Engineering: Basic Concepts*, 2nd ed.; Prentice Hall: Upper Saddle River, NJ, 2001.

(20) Lui, W.; Lee, C. Practical identification analysis of haldane kinetic parameters describing phenol biodegradation in batch operations. *J. Environ. Eng. Manage.* **2007**, *17* (1), 71-80.

(21) Berggren, D. R. V. Kinetic and Molecular Effects of Sulfate Reduction on a Dechlorinating Culture under Chemostat Growth Conditions. Masters of Science, Oregon State University, Corvallis, OR, September 21, 2011.

(22) Yu, S.; Dolan, M. E.; Semprini, L. Kinetics and Inhibition of Reductive Dechlorination of Chlorinated Ethylenes by Two Different Mixed Cultures. *Environ. Sci. Technol.* **2005**, *39*, 195-205.

(23) Azizian, M. F. Oregon State University, Corvallis, OR. Unpublished work, 2015.

(24) Haston, Z. C.; McCarty, P. L. Chlorinated Ethene Half-Velocity Coefficients (KS) for Reductive Dechlorination. *Environ. Sci. Technol.* **1999**, *33* (2), 223-226.

(25) Mayer-Blackwell, K. Stanford University, Stanford, CA. Private communication, 2016.

(26) Gossett, J. M. Measurement of Henry's Law Constants for C_1 and C_2 Chlorinated Hydrocarbons. *Environ. Sci. Technol.* **1987**, *21* (2), 202-208.

(27) Staudinger, J.; Roberts, P. V. A critical compilation of Henry's law constant temperature dependence relations for organic compounds in dilute aqueous solutions. *Chemosphere.* **2000**, *44* (4), 561-576.

(28) Mackay, D.; Shiu, W. Y. A Critical Review of Henry's Law Constants for Chemicals of Environmental Interest. *J. Phys. Chem. Ref. Data* **1981**, *10* (4), 1175-1199.

(29) Award Abstract #1330832 - Dynamics of Reductive Dehalogenating Communities Associated with Dehalorespiration Under Conditions of Competition for Hydrogen. http://www.nsf.gov/awardsearch/showAward?AWD_ID=1330832 (accessed June 26, 2015).

APPENDICES

Appendix A. Nomenclature

CAH	Chlorinated aliphatic hydrocarbon
cis-DCE	*cis*-Dichloroethene, *cis*-Dichloroethylene
Chemostat	*See* "CSTR"
C_L	Liquid concentration
$C_{L,y}$	Liquid concentration of inhibitor *y*
$C_{L,z}$	Liquid concentration of substrate *z*
CSTR	Continuously-stirred tank reactor
DI	Deionized
DNAPL	Dense non-aqueous phase liquid
ETH	Ethene, Ethylene
EV2L	EV culture in 2-L reactor
EV5L	EV culture in 5-L reactor
FID	Flame ionization detector
GC	Gas chromatograph
H_{CC}	Dimensionless Henry's Law constant
$H_{CC,z}$	Dimensionless Henry's Law constant for substrate *z*
H_{pc}	Pressure-concentration Henry's Law constant
$K_{corrected,z}$	Correction factor for substrate *z*
$K_{cor,z}$	See "$K_{corrected,z}$"
K_I	Inhibition constant
$K_{I,y}$	Inhibition constant for inhibitor *y*
k_m	Maximum specific utilization rate
$k_{m,z}$	Maximum specific utilization rate of substrate *z*
k_mX	Maximum utilization rate
K_S	Half-saturation constant
$K_{S,z}$	Half-saturation constant for substrate *z*
M_{TCE}	Mass of TCE within the reactor

M_z	Mass of substrate z
NSF	National Science Foundation
PCR	Polymerase chain reaction
PM	Point Mugu
R^2	Coefficient of determination
S	Substrate concentration
SSE	Sum of squared errors
TCE	Trichloroethene, Trichloroethylene
VC	Vinyl chloride
V_G	Reactor headspace volume
V_L	Reactor liquid volume
X	Biomass concentration
Y	Yield coefficient
μ	Specific growth rate
μ_m	Maximum specific growth rate

Appendix B. Henry's Law Constants

TCE and *cis*-DCE H_{CC} values from Table B.1 are used in all raw data analyses to convert gas concentrations measured by the GC to total reactor masses. The calculated VC H_{CC} value of 0.9030 using the coefficients determined by Gossett (1987) was not used; a value of 0.956 was used instead and its origin is unknown. The calculated VC H_{CC} value of 0.946 using the coefficients determined by Staudinger & Roberts (2000) is similar, but not the exact value used in spreadsheet calculations. Spreadsheets for experimental data analysis were passed down from previous students and the process of confirming Henry's Law constant values with literature was neglected.

Table B.1. Summary of empirical coefficients to determine Henry's Law constants for different compounds at a desired temperature and the resulting H_{pc} and H_{CC} values for CAHs used in this study (*26*). Values were determined at T = 20 °C (293 K). All H_{CC} values calculated in this manner should have been used in this study, but were not.

	$H_{pc} = e^{(A - B/T)}$			$H_{CC} = H_{pc}/RT$	
Compound	*A*	*B*	R^2	H_{pc} (m^3-atm/mol)	H_{CC}
TCE	11.37	4780	0.996	0.0071	0.2964
cis-DCE	8.47	4192	0.979	0.0029	0.1224
VC	7.385	3286	0.987	0.0217	0.9030

The recommended ethene H_{CC} value is 8.9 at T = 20 °C (293 K) but a value of 8 was used by previous students and was also not confirmed (*28*). Values from literature and values used in data analyses are not significantly different and do not impact the final results of this study.

Appendix C. Supporting Calculations

Confirm reaction stoichiometry:

TCE to *cis*-DCE	$HC_2Cl_3 + H_2 \rightarrow H_2C_2Cl_2 + HCl$
cis-DCE to VC	$H_2C_2Cl_2 + H_2 \rightarrow H_3C_2Cl + HCl$
VC to ethene	$H_3C_2Cl + H_2 \rightarrow C_2H_4 + HCl$
Net reaction	$HC_2Cl_3 + 3H_2 \rightarrow C_2H_4 + 3HCl$

Required H_2 to completely transform 10 mM TCE to ethene:

$$(10\ mM\ TCE)\left(\frac{3\ mM\ H_2}{mM\ TCE}\right) = \boxed{30\ mM\ H_2}$$

Required H_2 to completely transform TCE at the aqueous solubility limit to ethene (*16*):

$$\left(\frac{1100\ mg\ TCE}{L}\right)\left(\frac{g\ TCE}{1000\ mg\ TCE}\right)\left(\frac{mol\ TCE}{131.4\ g\ TCE}\right)\left(\frac{1000\ mmol\ TCE}{mol\ TCE}\right)\left(\frac{3\ mmol\ H_2}{mmol\ TCE}\right) = \boxed{25.1\ mM\ H_2}$$

Appendix D. Supporting Figures

Examples of experimental mass vs. time data and the application of the Multi-Fit Monod Model to that experimental data are provided to support the predictive capabilities of the theoretical model.

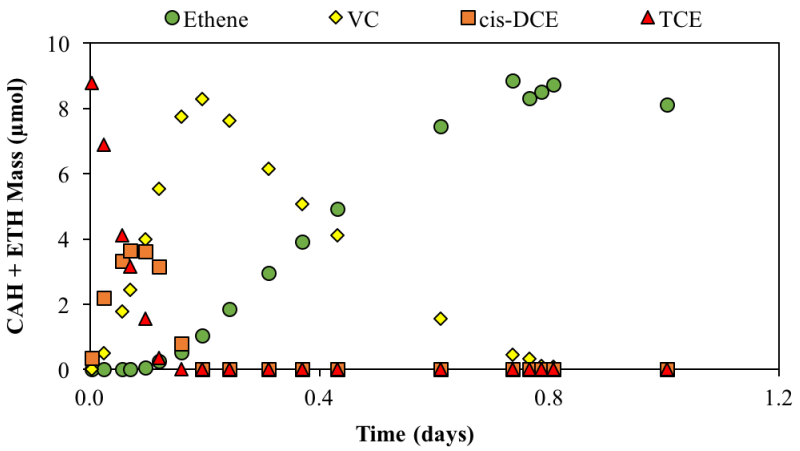

Figure D1. Example of CAH mass over time data for batch kinetic test on EV2L culture.

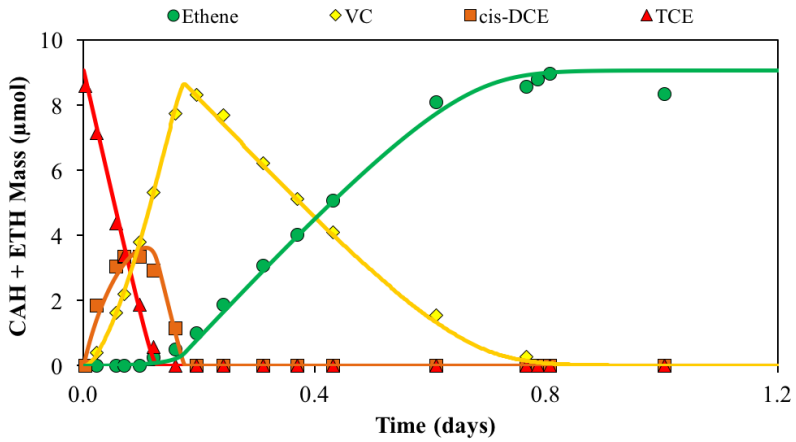

Figure D2. Example of Multi-Fit Monod Model applied to CAH mass over time data for batch kinetic test on EV2L culture.

CAH transformation rates have been monitored in all chemostats for many years. Most recent data for 2013-2015 is presented to show natural fluctuations over time. Seasonal temperature changes and natural microbial community shifts over time have the largest impact on these transformation rates. All k_mX values were determined using the Multi-Fit Monod Method.

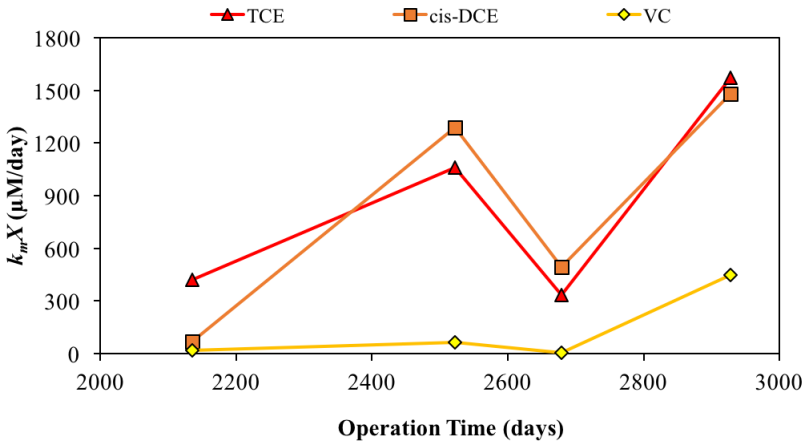

Figure D3. Average CAH rates in EV2L over three-year time period (2013-2015). Natural fluctuations occur as a result of temperature changes and microbial community shifts over time. Sharp increase in rates after 2800 days is the result of formate increase.

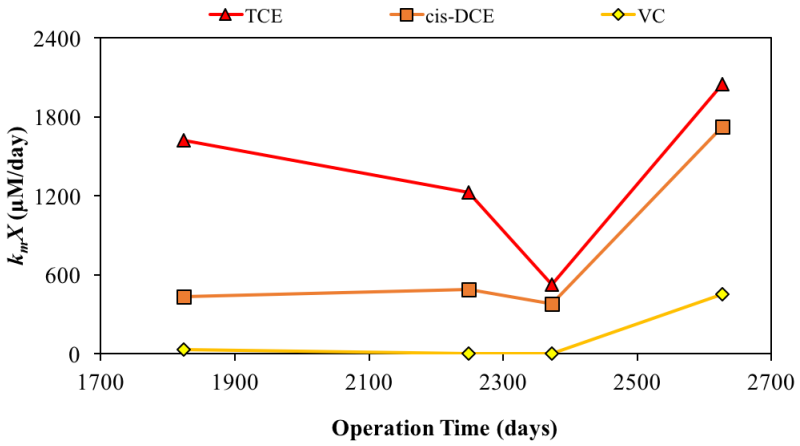

Figure D4. Average CAH rates in VS2L over three-year time period (2013-2015). Natural fluctuations occur as a result of temperature changes and microbial community shifts over time. Sharp increase in rates after 2500 days is the result of formate increase.

VS2L k_mX values are presented with 95% confidence intervals included to show that fluctuations in rates during transient electron donor concentration experiments are slightly less pronounced. There are no explanations for the k_mX decrease at day 2575.

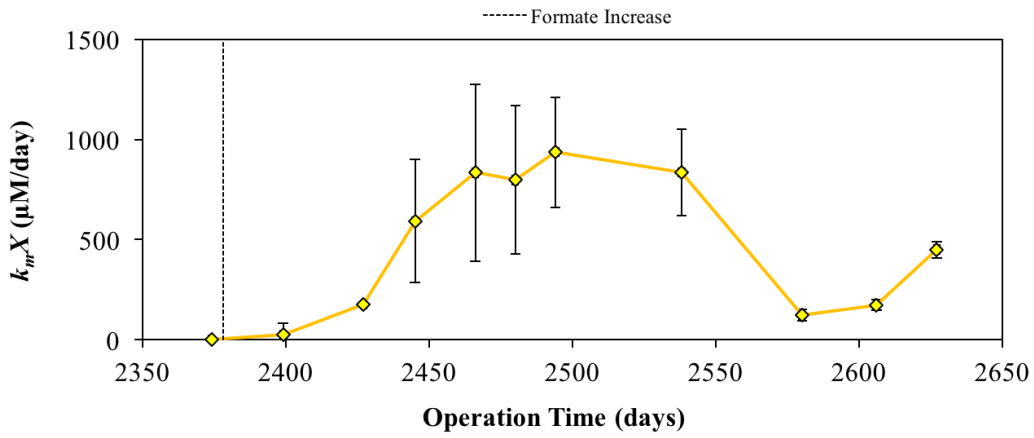

Figure D5. VS2L VC k_mX values during transient electron donor concentration experiments. Error bars represent 95% confidence intervals. Fluctuations in rates are slightly less pronounced when confidence intervals are included. There are no explanations for k_mX decrease at day 2575.

The method of rate analysis had an effect on the CAH transformation rate determined. "Converted linear rates" determined using the linear rate method were consistently lower than "kmX" values determined using the Multi-Fit Monod Model because the linear method does not account for the competitive inhibition observed in these cultures.

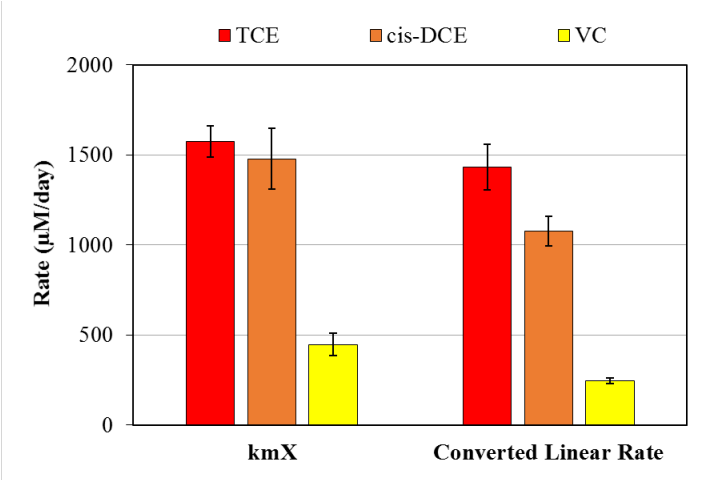

Figure D6. Example of how average transformation rates differ depending on rate analysis method used. "kmX" values were determined using Multi-Fit Monod Model, while "Converted Linear Rate" values were determined using linear rate method. Error bars represent 95% confidence intervals.

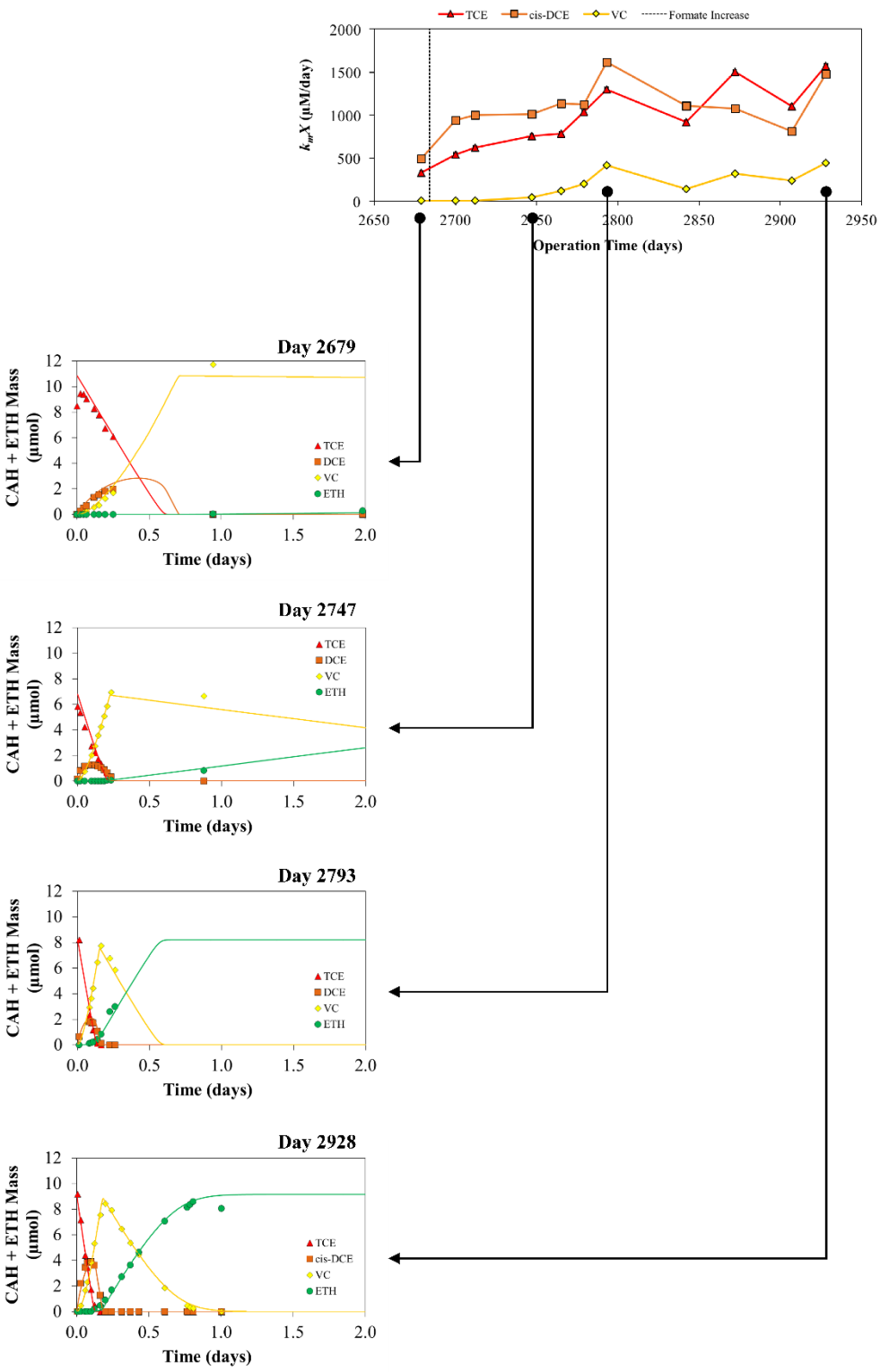

Figure D7. Comparison of Multi-Fit Monod Model fitting for EV2L during transient electron donor concentration experiments. TCE and VC rates show most pronounced increase over time, stabilizing near the conclusion of experiments when the reactor reached steady state operation.

Headspace and reactor solution monitoring is ongoing for all chemostats in operation. Acetate and H_2 was tracked in EV5L and VS5L during transient electron donor concentration experiments. Steady state conditions for 2L cultures were compared to steady state conditions for 5L cultures.

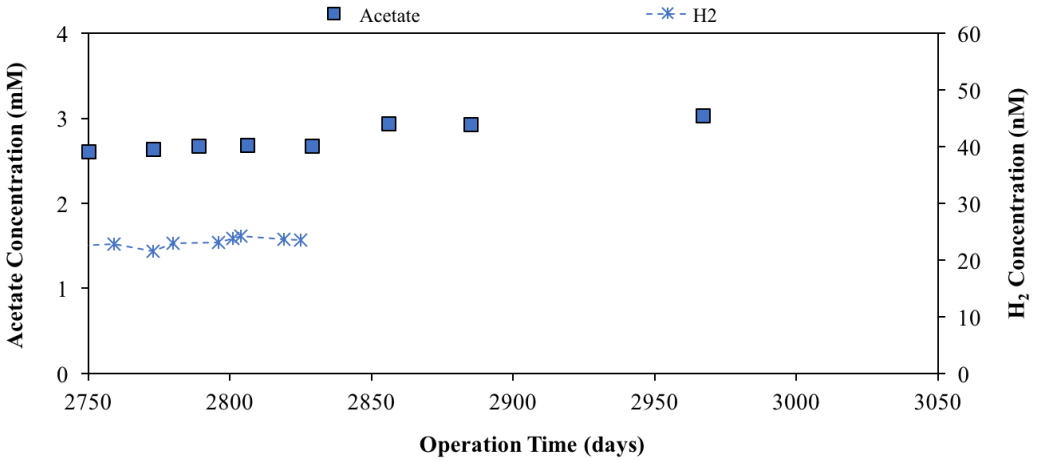

Figure D8. Acetate and H_2 concentration monitoring in EV5L during transient electron donor concentration experiments. H_2 concentrations in EV2L at steady state were much higher than EV5L, but acetate concentrations were comparable.

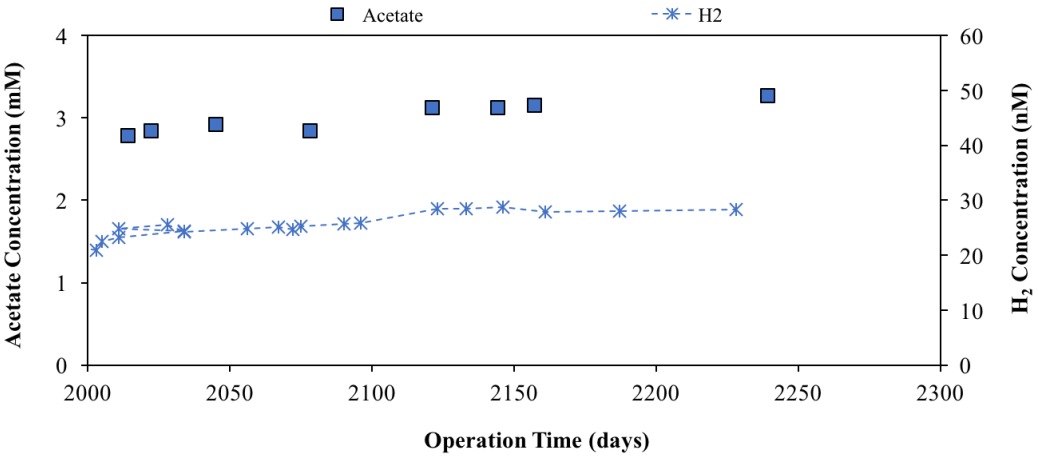

Figure D9. Acetate and H_2 concentration monitoring in VS5L during transient electron donor concentration experiments. H_2 concentrations in VS2L at steady state were much higher than VS5L, but acetate concentrations were comparable.

Appendix E. National Science Foundation Grant

The research presented in this study was a registered contribution to the National Science Foundation (NSF) Molecular and Cellular Biosciences (MCB) Grant No. 1330832 titled "Dynamics and Reductive Dehalogenating Communities Associated with Dehalorespiration Under Conditions of Competition for Hydrogen." Facilitated by Principal Investigators Dr. Lewis Semprini and Dr. Alfred Spormann, this collaborative research aimed to explore various properties of dehalogenating microbes and create a mathematical model able to predict competition for hydrogen within the microbial community. The research facilitated by this grant had three aspects of broader impact. The first aspect was successful application of this reductive dehalogenation process for bioremediation purposes in areas of significant groundwater contamination with chlorinated solvents. The second aspect was the fundamental understanding of the biology of *Dehalococcoides* spp. and similar microbes through investigation into the "physiological dynamics and natural population structure." The third and final aspect was the development and training of a future generation of microbiologists and environmental engineers through active contribution to the funded research (*29*).

This research played a role in the improvement of the mathematical model in place to predict dehalogenation processes within mixed anaerobic cultures, as well as in the expansion of knowledge about *Dehalococcoides* spp. through extensive kinetic analysis. The work required to complete this research tied into the broader impacts of this NSF grant by providing insight into the microbial kinetic parameters and abilities of these cultures and by expanding the technical skills and critical thinking abilities of the Contributor by means of mentored projects.